On Hyperbolic evolution equations: Theory and Numerics

Ujjwal Koley

Dissertation presented for the degree
of Philosophiæ Doctor

Department of Mathematics
University of Oslo
2010

Series of dissertations submitted to the
Faculty of Mathematics and Natural Sciences, University of Oslo
No. 1007

ISSN 1501-7710

Cover: Inger Sandved Anfinsen.
Printed in Norway: AiT e-dit AS.

Produced in co-operation with Unipub.
The thesis is produced by Unipub merely in connection with the
thesis defence. Kindly direct all inquiries regarding the thesis to the copyright
holder or the unit which grants the doctorate.

Preface

This is a thesis for the degree of Philosophiæ Doctor, and consists of four research papers preceded by an introductory note. The introductory part describes the necessary background material and summarises the papers. The research articles reported here, are written in the course of last three years while being employed at Centre of Mathematics for Applications, University of Oslo.

In memory of my beloved sister..

Acknowledgements

The writing of a dissertation in a distant land, far far away from home, can be a lonely and isolating experience, yet it is obviously not possible without the personal and practical support of numerous people.

First and foremost, I voice my manifold respect and sincere appreciation to my supervisor, Prof. Nils Henrik Risebro. With his enthusiasm, his inspiration, and his great efforts to explain things clearly and simply, he helped to make mathematics fun for me. Its a pleasure to thank my second supervisor Prof. Magnus Svärd for all his very useful suggestions and the valuable discussions that I have had with him.

I also express my sincere thanks to Prof. Kenneth Hvistendahl Karlsen, who donated his time and expertise to help me learn the deep insight of conservation laws theory. I am thankful to Prof. Siddhartha Mishra for introducing me to the numerical aspects of conservation laws and guiding me to solve many real life problems as well.

The Centre of Mathematics for Applications, lead by Prof. Ragnar Winther and Helge Galdal, provided an excellent academic work place. I have the highest regard for both of them. My graduate studies would not have been the same without the social and academic challenges and diversions provided by all my colleagues at the institute, with special thanks to Franz Georg Fuchs, Asma Khedher, Yeliz Yolcu Okur, Andrew D. McMurry, Trygve Karper. Special thanks to Dr. Imran Habib Biswas for convincing me that I can also stay in Norway during winter time! I fondly remember all the academic and non-academic discussions that I have had with him.

Before moving abroad, I was privileged to complete a master degree in Mathematics at the TIFR Centre for Applicable Mathematics. I am greatful to all my teachers at TIFR Centre. In particular, I would like to thank my master's supervisor Prof. Veerappa Gowda for his valuable suggestions and constant encouragement. The memories of all the good time I had with friends are still very much alive, and I am specially thankful to Rajib, Shirshendu, Prosenjit, Kaushik for that. I owe a lot to all my teachers at Ramakrishna Mission Residential College, which opened up the world for me.

I also thank my 'non-mathematical' friends: All the members of our cricket club, for giving me a feeling of being rooted, at home. It is an honour to share the same dressing room with these cricket stars.

Finally, and very personally, I express my sincere thanks to my parents, and my siblings for all their support and encouragements.

Oslo, July 2010 Ujjwal Koley.

Table of Contents

1 Introduction **1**
1.1 Hyperbolic Equations 1
1.2 Degenerate Convection-Diffusion Equations 5
1.3 Nonlinear Dispersive Equations 7
1.4 Numerical method for PDEs 10
1.5 Magnetic Induction Equations 16
1.6 Magnetic induction equations with resistivity 19
1.7 Summary of Paper I 21
1.8 Summary of Paper II 23
1.9 Summary of Paper III 25
1.10 Summary of Paper IV 30
1.11 Concluding remarks 36

2 Magnetic Induction equation **41**
U. Koley, S. Mishra, N. H. Risebro, M. Svärd
BIT Numer Math (2009) 49:375-395
2.1 Introduction 41
2.2 The Continuous problem 45
2.3 Semi-discrete Schemes 48
2.4 Numerical Experiments 51
2.5 Conclusion 60

3 Magnetic Induction equation with resistivity **63**
U. Koley, S. Mishra, N. H. Risebro, M. Svärd
IMA Journal of Numerical Analysis, to appear
3.1 Introduction 63
3.2 The Continuous problem 66
3.3 Semi-discrete Schemes 68
3.4 Schemes in Three-dimensions 75
3.5 Numerical Experiments 76

3.6 Conclusion 83

4 Kawahara Equation **89**
U. Koley
Submitted
4.1 Introduction 89
4.2 Semi-discrete Analysis 91
4.3 Fully-discrete semi-Implicit Scheme 99
4.4 Uniqueness 105
4.5 Numerical experiments 105

5 Rate of convergence **111**
K. H. Karlsen, U. Koley, and N.H. Risebro
Submitted
5.1 Introduction 111
5.2 Preliminaries 113
5.3 Proof of the main theorem 117
5.4 A numerical test 131

1 Introduction

This thesis consists of four papers, and they are summarised in this introductory part. The first part of the thesis deals with the induction equations, which is a submodel of ideal magneto-hydrodynamics (MHD) equations. The equations of ideal MHD describe the evolution of macroscopic plasmas, and arise in many other contexts in astrophysics, and electrical and aerospace engineering. Being a non-strict hyperbolic system, the solution structure of MHD equations is fairly complex.

Given the formidable difficulties of the full MHD system, we consider the magnetic induction equations as a model. Since these equations appear as a sub-model in the MHD equations, the design of stable and high-order accurate numerical schemes for the induction equations can lead to the design of robust schemes for the non-linear MHD equations. In first two papers (papers I-II), we design stable and high order accurate finite difference schemes for initial-boundary value problems corresponding to the magnetic induction equations and magnetic induction equations with resistivity (sub-model of MHD equations with resistivity) respectively. In paper-III, we consider Korteweg-de Vries-Kawahara (Kawahara) equation, which is a form of the Korteweg-de Vries (KdV) equation with an additional fifth order term. We considered both the semi-discrete as well as fully-discrete schemes for the initial-boundary value problem corresponding to the Kawahara equation. Convergence of both schemes has been shown in this paper. Finally, in paper-IV, we consider semi-discrete first-order finite difference schemes for a nonlinear degenerate convection-diffusion equations in one space dimension, and prove an L^1 error estimate.

1.1 Hyperbolic Equations

Hyperbolic partial differential equations arise in a broad spectrum of disciplines where wave motion or advective transport is important; gas dynamics, acoustics, elastodynamics, optics, geophysics, and biomechanics, to name but a few. Specially, the second half of the XXth century has seen enormous progress in the application of the techniques of functional analysis to investigate in a mathematical rigorous way the properties of solutions to nonlinear partial differential equations and systems appear in the different branches of continuum physics. As a rule, functions vital for the considered problems are

not smooth enough to satisfy these equations in the classical sense. Thus, there arises the need to introduce a notion of a generalized solution and to develop theory and numerical methods for constructiong these solutions.

1.1.1 Scalar conservation laws

Initial value problem for hyperbolic scalar conservation laws are partial differential equations of the following form:

$$u_t + f(u)_x = 0, \quad u|_{t=0} = u_0. \tag{1.1.1}$$

If we formally integrate equation (1.1.1) between two points x_1 and x_2, we obtain

$$\int_{x_1}^{x_2} u_t \, dx = -\int_{x_1}^{x_2} f(u)_x \, dx = f(u(x_1,t)) - f(u(x_2,t)).$$

Assuming that u is sufficiently regular to allow us to take the derivative outside the integral, we get

$$\frac{d}{dt}\int_{x_1}^{x_2} u(x,t) \, dx = f(u(x_1,t)) - f(u(x_2,t)). \tag{1.1.2}$$

This equation expresses conservation of the quantity measured by u in the sense that the rate of change in the amount of u between x_1 and x_2 is given by the difference in $f(u)$ evaluated at these points.

Assuming that the solution u is smooth, one can find u along the characteristics given by $x = x_0 + f'(u_0(x_0))t$. It is well known that no matter how smooth the initial function is, we cannot expect to be able to define classical solutions of nonlinear conservation laws for all time. In this case we have to extend the concept of solutions in order to allow discontinuities. Therefore we need to consider (1.1.1) in integral form. We consider test functions in the space $C_c^\infty(\mathbb{R} \times [0,\infty))$ consisting of the smooth functions with compact support in $\mathbb{R} \times [0,\infty)$.

Definition 1.1.1. *(Weak solution) A function $u \in L^1(\mathbb{R} \times [0,\infty))$ is a weak solution of (1.1.1) if for any such test function $\phi \in C_c^\infty(\mathbb{R} \times [0,\infty))$, we have*

$$\int_{-\infty}^{\infty}\int_{0}^{\infty} (u\phi_t + f(u)\phi_x) \, dt \, dx + \int_{-\infty}^{\infty} \phi(x,0)u_0(x) \, dx = 0. \tag{1.1.3}$$

Observe in particular that a (regular) smooth solution is a weak solution as well. It is now natural to ask what kind of discontinuities are compatible with (1.1.3)? The precise answer is the following: A discontinuity in u connecting two states u_l and u_r must travel with a speed σ given by the **Rankine-Hugoniot** condition

$$\sigma(u_l - u_r) = f(u_l) - f(u_r).$$

Although in case of hyperbolic equations, due to the loss of regularity, it is necessary to work with weak solutions but due to neglected physical (e.g., dissipative) mechanisms weak solutions are not uniquely determined by their data. For these reasons attention

focuses on finding a physically reasonable framework which incorporates discontinuous solutions and ensures uniqueness and they are commonly referred to as **"entropy conditions".**

One of the most common entropy conditions is so-called viscous regularization, where the scalar conservation law $u_t + f(u)_x = 0$ is replaced by $u_t + f(u)_x = \epsilon u_{xx}$. The idea is that the physical problem has some diffusion, and that the conservation law represents a limit model when the diffusion is small. Based on this, one looks for solutions of the conservation laws that are limits of the regularized equation when $\epsilon \to 0$. Choose a smooth convex function $\eta = \eta(u)$ and a nonnegative test function ϕ in $C_c^\infty(\mathbb{R} \times (0, \infty))$. (Such a test function will be supported away from the x-axis , and thus we get no contribution from the initial data.) Then we find

$$\begin{aligned}
0 &= \iint (u_t + f(u)_x - \epsilon u_{xx})\eta'(u)\phi \, dx \, dt \\
&= \iint \eta(u)_t \phi \, dx \, dt + \iint q'(u) u_x \phi \, dx \, dt \\
&\quad - \epsilon \iint \left(\eta(u)_{xx} - \eta''(u)(u_x)^2 \right) \phi \, dx \, dt \\
&= - \iint \eta(u)\phi_t \, dx \, dt - \iint q(u)\phi_x \, dx \, dt \\
&\quad - \epsilon \iint \eta(u)\phi_{xx} \, dx \, dt + \epsilon \iint \eta''(u)(u_x)^2 \phi \, dx \, dt \\
&\geq - \iint (\eta(u)\phi_t + q(u)\phi_x + \epsilon \eta \phi_{xx}) \, dx \, dt,
\end{aligned}$$

where we first introduced q such that

$$q'(u) = f'(u)\eta'(u)$$

and subsequently used the convexity of η, i.e., $\eta'' \geq 0$. Interpreted in a distributional sense we may write this as

$$\frac{\partial}{\partial t}\eta + \frac{\partial}{\partial x} q \leq \epsilon \eta_{xx}.$$

If this is to hold as $\epsilon \to 0$, then

$$\frac{\partial}{\partial t}\eta + \frac{\partial}{\partial x} q \leq 0.$$

Definition 1.1.2. *(Entropy inequality). A weak solution u satisfies the* **entropy inequality** if for any convex function η with $\eta_u f_u = q_u$

$$\int_{-\infty}^{\infty} \int_0^{\infty} (\eta(u)\phi_t + q(u)\phi_x) \, dx \, dt \geq 0, \tag{1.1.4}$$

for all test functions $\phi \in C_c^\infty(\mathbb{R} \times (0, \infty))$ with $\phi(x, t) \geq 0 \ \forall x, t$.

This weak entropy inequality chooses the physically relevant solution among all the weak solutions.

For the scalar equation, one can show existence, uniqueness and continuous dependence on data of the entropy solution when u_0 has bounded total variation (TV). Then we have that $TV(u) \leq TV(u_0)$. The viscous approximation u_ϵ, given by solving

$$\partial_t u_\epsilon + \partial_x f(u_\epsilon) = \epsilon \partial_x^2 u_\epsilon, \quad u_\epsilon|_{t=0} = u_0, \quad \epsilon \geq 0 \tag{1.1.5}$$

then converges to the entropy solution as $\epsilon \to 0$. The proofs of stability rely on the technique of **"doubling of variables"** due to Kruzkov, see for example [1] for an account. There is also an existence result for solutions in L^∞ based on **"compensated compactness"**.

1.1.2 Systems of conservation laws

We now consider the system of conservation laws

$$\mathbf{u}_t + f(\mathbf{u})_x = 0, \quad \mathbf{u}\,|_{t=0} = \mathbf{u}_0, \tag{1.1.6}$$

where $\mathbf{u}$ and f are in $\mathbb{R}^m$. If the Jacobian $f'(\mathbf{u})$ has only real eigenvalues $\lambda_1, \cdots, \lambda_m$, also called the characteristic speeds, the system is called hyperbolic, and if the eigenvalues are distinct for any $\mathbf{u}$, it is called strictly hyperbolic.

Linear hyperbolic equations

The easiest case of the hyperbolic conservation laws (1.1.6) is, when the flux function f is linear, i.e.,

$$\mathbf{u}_t + A\mathbf{u}_x = 0, \quad A \in \mathbb{R}^{m \times m}. \tag{1.1.7}$$

The equation (1.1.7) is called hyperbolic if A is diagonalizable with real eigenvalues. For a linear hyperbolic PDE there exist eigenvalues $\lambda_1 \leq \cdots \leq \lambda_m$ and a complete set of eigenvectors $r^1, \cdots, r^m \in \mathbb{R}^m$, such that $R = [r^1 \mid \cdots \mid r^m]$ is non-singular. By multiplying (1.1.7) with R^{-1}, we can rewrite this linear system as

$$R^{-1}\mathbf{u}_t + R^{-1}ARR^{-1}\mathbf{u}_x = 0.$$

Introducing the so-called **characteristic variables** $\mathbf{w}(x,t) := R^{-1}\mathbf{u}(x,t)$ we can rewrite the linear equation as

$$\mathbf{w}_t + \Lambda \mathbf{w}_x = 0,$$

where $\Lambda = \text{diag}(\lambda_1, \cdots, \lambda_m)$. Using the characteristic variables, we can see that the linear system decouples into m independent advection equations

$$\mathbf{w}_t^p + \lambda_p \mathbf{w}_x^p = 0, \quad p = 1, 2, ..., m.$$

Now we can solve the linear system (1.1.7) together with the initial condition $\mathbf{u}(x,0) = \mathbf{u}_0(x)$. The solution consists of m "waves" travelling at characteristic speeds λ_p

$$\mathbf{u}(x,t) = \sum_p \mathbf{w}^p(x,t) r^p = \sum_p \mathbf{w}_0^p(x - \lambda_p t) r^p.$$

Non-linear Systems

In the case of a linear hyperbolic system of m equations, we know that for a solution there are at any point x exactly m waves passing by at different speeds, and we observe a superposition of these waves. In the nonlinear case, these waves are constantly interacting with each other, and in addition they deform separately. These problems cannot be solved analytically in general.

An isolated discontinuity can be called a shock related to the characteristics field i if it travels with speed σ such that $\lambda_i(\mathbf{u}_r) < \sigma < \lambda_i(\mathbf{u}_l)$, and that either $\sigma > \lambda_j(\mathbf{u})$ or $\sigma < \lambda_j(\mathbf{u})$ on both sides for $j \neq i$. A contact discontinuity related to the characteristic field satisfies $\lambda_i(\mathbf{u}_r) = \sigma = \lambda_i(\mathbf{u}_l)$. If $\lambda_i'(\mathbf{u}).r_i(\mathbf{u}) = 0$, where r_i is the right eigenvector associated to λ_i, a contact discontinuity is the only possibility. In that case we say that the characteristic field i is linearly degenerate. If it is never the case, the characteristic field is genuinely nonlinear. Other types of waves that occur in the solution of the Riemann problem of (1.1.6) are rarefractions and compound waves containing over-or undercompressive shocks. The latter only occurs if there are characteristic fields which are neither linearly degenerate nor genuinely nonlinear.

1.2 Degenerate Convection-Diffusion Equations

In this section, we will consider nonlinear, possibly strongly degenerate, convection diffusion equations of the form

$$\begin{cases} u_t + f(u)_x = A(u)_{xx}, & (x,t) \in \Pi_T, \\ u(0,x) = u_0(x), & x \in \mathbb{R}, \end{cases} \tag{1.2.1}$$

where $\Pi_T = \mathbb{R} \times (0,T)$ with $T > 0$ fixed. $u(x,t)$ denotes the (scalar) unknown, $u_0(x)$ is a given function of bounded variation, $f(u)$ and $A(u)$ are given locally smooth bounded functions. Regarding A, the basic assumption is that $A'(u) \geq 0$ and thus (1.2.1) is a strongly degenerate parabolic problem.

Convection-diffusion equations arise in a variety of applications, among others turbulence, traffic flow, financial modelling and front propagation. Such equations also constitute an important part of a system of equations describing two phase flow in oil reservoirs [6] as well as a system of equations describing sedimentation processes used for solid-liquid separation in industrial applications [4, 5]. When (1.2.1) is non-degenerate, i.e., $A'(u) > 0$, it is well known that (1.2.1) admits a unique classical solution [7]. This contrasts with the case where (1.2.1) is allowed to degenerate at certain points, i.e., $A'(u)$ may vanish for some values of u. Solutions are then not necessarily smooth, and weak solutions must be sought.

Definition 1.2.1. *(Weak Solution). A function $u(x,t)$ is called a weak solution if, for all suitable test functions ϕ, it satisfies*

$$\int_{\mathbb{R}} \int_0^T (u\phi_t + f(u)\phi_x + A(u)\phi_{xx})\, dx\, dt + \int_{\mathbb{R}} u_0(x)\phi(x,0)\, dx = 0. \tag{1.2.2}$$

The simplest examples of degenerate equations are perhaps provided by the porous medium equation $u_t = (u^m)_{xx}$, $m > 1$ and the convective porous medium equation $u_t + (u^n)_x = (u^m)_{xx}$, $n, m > 1$, which both degenerate at $u = 0$. A striking manifestation of this one-point degeneracy is finite speed of propagation. The reader who is interested in an overview of the very extensive literature that exists on degenerate parabolic problems is reffered to the papers [8, 9] and the references therein. We will from now on refer to (1.2.1) as **degenerate** when $A(u)$ is strictly increasing and **strongly degenerate** when $A(u)$ is merely non-decreasing.

In the strongly degenerate case there exist two numbers α and β such that $A'(u) = 0$ on the interval $[\alpha, \beta]$. A simple example of a strongly degenerate equation is a hyperbolic conservation law $u_t + f(u)_x = 0$. Thus (1.2.1) must in general possess discontinuous solutions. Furthermore, discontinuous solutions defined by an integral equality (1.2.2) is not uniquely determind by their data. In fact, an additional condition - an entropy condition is needed to single out the physically relevant weak solution.

Lemma 1.2.1. *Suppose that $A'(u) \geq \alpha > 0$ and let $u(x,t)$ denote the unique classical solution of the parabolic problem* (1.2.1)*. Let $\eta : \mathbb{R} \to \mathbb{R}$ be a C^2 convex entropy function and q, r the associated entropy fluxes satisfying the compatibility conditions*

$$q'(u) = \eta'(u)f'(u), \quad r'(u) = \eta'(u)A'(u). \tag{1.2.3}$$

Then for all suitable test functions $\phi \geq 0$,

$$\iint \left(\eta(u)\phi_t + q(u)\phi_x + r(u)\phi_{xx}\right)\, dx\, dt \geq 0$$

Proof. Multiply (1.2.1) by $\eta'(u)$ and use the chain rule, we get

$$\eta(u)_t + \eta'(u)f'(u)u_x = \eta'(u)A(u)_{xx}$$

Using integration by parts, the compatibility conditions (1.2.3) and the convexity of η to throw away the dissipative mechanisms, we obtain

$$\begin{aligned}
0 &= \iint \left(\eta(u)_t + \eta'(u)f'(u)u_x - \eta'(u)A(u)_{xx}\right)\, dx\, dt \\
&= \iint \left(-\eta(u)\phi_t - q(u)\phi_x + A(u)_x(\eta'(u)\phi)_x\right)\, dx\, dt \\
&= \iint \Big(-\eta(u)\phi_t - q(u)\phi_x + A'(u)u_x(\eta''(u)u_x\phi + \eta'(u)\phi_x)\Big)\, dx\, dt \\
&= \iint \Big(-\eta(u)\phi_t - q(u)\phi_x + A'(u)\eta''(u)(u_x)^2\phi - r(u)\phi_{xx})\Big)\, dx\, dt \\
&\geq \iint \left(-\eta(u)\phi_t - q(u)\phi_x - r(u)\phi_{xx})\right)\, dx\, dt,
\end{aligned}$$

from which the lemma follows. □

In view of the previous lemma, we have the following inequality weakly:

$$\eta(u)_t + q(u)_x - r(u)_{xx} \leq 0,$$

for all convex C^2 entropies $\eta : \mathbb{R} \to \mathbb{R}$ and corresponding fluxes q, r. By a limiting argument, we can let $\eta(u) \to |u-k|$, for any given $k \in \mathbb{R}$, and use $q(u) = sign(u-k)(f(u)-f(k))$ and $r(u) = |A(u)-A(k)|$. We now introduce the following definition of an entropy weak solution of (1.2.1):

Definition 1.2.2. *A weak solution $u(x,t)$ of (1.2.1) is called an entropy solution if, for all real numbers k and suitable test functions $\phi \geq 0$,*

$$\iint (|u-k|\phi_t + sign(u-k)(f(u)-f(k))\phi_x + |A(u)-A(k)|\phi_{xx})\, dx\, dt \geq 0$$

For scalar conservation laws, the entropy framework (usually called entropy conditions) was introduced by Kružkov [13] and Vol'pert [14], while for degenerate parabolic equations entropy solution were first considered by Vol'pert and Hudajev [15]. Uniqueness of entropy solutions to (1.2.1) was first proved by Carrillo [11], see also Karlsen and Risebro [12]. On the other hand, the uniqueness of weak solutions for the purely parabolic case (no convection term) in the class of bounded integrable functions has been proved by Brezis and Crandall [10].

1.3 Nonlinear Dispersive Equations

In the last thirty years, the theory of nonlinear evolution equations has grown into a large field that attracts the attention of both mathematicians and physicists in view of its applications to real world nonlinear models and of the novelty of the problems. It is intended to be a new source for modern research dealing with nonlinear phenomena of dispersive type. One of the reasons these equations are called **dispersive** is that the solution of these equations are waves that spread out spatially as long as no boundary conditions are inposed.

The central equations of study in this thesis are model equations for waves which take account of both nonlinearity and dispersion effects. For example, by modelling equations for waves in dispersion media, we begin by considering a body of water of finite depth under the influence of gravity, bounded below by an impermeable surface. Ignoring the effects of viscosity and assuming that the flow is incompressible and irrotational, the motion is taken to be governed by the Euler equations together with suitable boundary conditions on the rigid surface and on the water-air interface. So, by making assumptions and approximations about the physical interest in question, we can obtain a set of model dispersive equations formally valid for the description of waves propagating in just one direction for small amplitude long wavelenth motion.

In this section, we will talk about two important examples of dispersive equations:

1.3.1 Korteweg-de Vries equation:

The Korteweg-de Vries (in short KdV) equation,

$$u_t + uu_x + u_{xxx} = 0, \tag{1.3.1}$$

has been studied extensively since its first analysis in 1895 by Korteweg and de Vries. This equation was considered by the above authors as a model for long water waves propagating in a channel. The significance of their ideas went more or less unappreciated for several decades. This can be traced in part to an inadequate description of their work by Lamb in his monumental treatise on hydrodynamics. The appearance of the same equation derived as a rudimentary model for waves in a number of diverse physical systems has awakened the interest of physicists and mathematicians. It is now generally understood that the Korteweg-de Vries equation, or other comparable model equations, can be expected to appear as describing to the first approximation the behaviour of unidirectional long waves in nonlinear dispersive media. More recently, the KdV equation has been found to describe wave phenomena in plasma physics, anharmonic crystals and bubble-liquid mixtures. The KdV equation is also relevant to the discussion of the interaction between nonlinearity and dispersion, just as the well-known Burgers equation shows the features of the interaction between nonlinearity and dissipation.

One fundamental mathematical representation of a wave moving in a one dimensional medium is given by functions of two variables $u(x,t)$ of the form

$$u(x,t) = \phi(x - ct) \tag{1.3.2}$$

where ϕ is a function of one variable and c is a nonzero constant. The animation of such a function begins with the graph of the initial profile $u(x,0) = \phi(x)$. If c is positive, then the profile of $u(x,t) = \phi(x - ct)$ at a large time t is exactly a translation of the initial profile by an amount ct in the positive x-direction. Such a function represents a disturbance moving with constant speed c. Similarly, $u(x,t) = \phi(x - ct)$ with $c < 0$, representing a disturbance moving in the negative x-direction with speed $|c|$. In either case, **the profile at each time t does not get distored and remains a recognizable feature of a wave as it is translated along x-axis.** Waves represented by functions of the form (1.3.2) are called **travelling waves.** Two basic features of any travelling wave are the underlying profile shape defined by ϕ and the speed $|c|$ at which the profile is translated along the x-axis.

Definition 1.3.1. Travelling wave solution: A travelling wave solution of a partial differential equation is a solution of the differential equation which has the form of a travelling wave $u(x,t) = \phi(x - ct)$, where c is the wave speed and $\xi = x - ct$ is the characteristic variable.

Definition 1.3.2. Solitary wave solution: This is the name given to a travelling wave solution when $\phi : \mathbb{R} \to \mathbb{R}$ satisfies the boundary conditions

$$\lim_{\xi \to \pm\infty} \phi^n(\xi) = 0$$

for all $n \in \mathbb{N}$.

In the case of a specific nonlinear evolution equation which is completely integrable, for example the KdV equation, the solitary wave solutions are called **solitons.** In general it is not obvious that travelling wave solutions exist for a speciifc model, but in case of KdV it does. An interesting fact, and rarely reffered to current literature, is that the

first mathematical proof of existence and uniqueness of solutions of the KdV equation was accomplished by Sjöberg [2] in 1970, using a finite difference approximation. His proof is valid for initial data that are periodic and with square integrable third derivative. Sjöberg's uniqueness proof still is the standard one, using the Gronwall inequality.

1.3.2 Korteweg-de Vries-Kawahara equation:

The Korteweg-de Vries-Kawahara (Kawahara in short) equation

$$u_t + uu_x + u_{xxx} = u_{xxxxx}, \tag{1.3.3}$$

occurs in the theory of magneto-acoustic waves in a plasmas and in the theory of water waves with surface tension. The Kawahara equation is an important nonlinear dispersive equation. It describes solitary wave propagation in media in which the first-order dispersion is anomalously small. Equation (1.3.3) was first proposed by Kawahara in 1972, as a model equation describing solitary-wave propagation in media. A more specific physical background of this equation was introduced by Hunter and Scheurle [3], where they used it to describe the evolution of solitary waves in fluids in which the Bond number is less than but close to $\frac{1}{3}$ and the Froude number is close to 1. In the literature this equation is also referred to as the fifth order KdV equation or singularly perturbed KdV equation. The fifth order term $\partial_x^5 u$ is called the Kawahara term.

It is well-known that KdV equation describes one dimensional waves of small but finite amplitude, but under certain circumstances, however, it might happen that the coefficient of the third order derivative in the KdV equation becomes small or even zero. In that case one has to take account of the higher order effect of dispersion in order to balance the nonlinear effect. In such cases one may obtain a generalized nonlinear dispersive equation, known as Kawahara equation, which has a form of the KdV equation with an additional fifth order derivative term given by (1.3.3). There has been a great deal of work on solitary wave solutions of the Kawahara equation [4, 5, 8, 10, 11] over the past thirty years. It is found that, similarly to the KdV equation, the Kawahara equation also has solitary wave solutions which decay rapidly to zero as $t \to \infty$, but unlike the KdV equation whose solitary wave solutions are non-oscillating, the solitary wave solutions of the Kawahara equation have oscillatory trails. This shows that the Kawahara equation is not only similar but also different from the KdV equation in the properties of solutions, like what happens between the formulations of this equation and the KdV equation. The strong physical background of the Kawahara equation and such similarities and differences between it and the KdV equation in both the form and the behavior of the solution render the mathematical treatment of this equation particularly interesting.

The Cauchy problem has been studied by a few authors [12, 13]. It has been shown that the problem has a local solution $u \in C([-T, T]; H^r(\mathbb{R}))$ if $f \in H^r(\mathbb{R})$ and $r > -1$. This local result combined with the energy conservation law yields that (1.3.3) has a global solution $u \in C([-\infty, \infty]; L^2(\mathbb{R}))$ if $f \in L^2(\mathbb{R})$. Well-posedness results can be found in [6].

1.4 Numerical method for PDEs

The subject of numerical schemes for hyperbolic conservation laws is quite well developed. Many schemes have been designed for both scalar and systems of conservation laws. Most of them approximate the solutions quite well although rigorous convergence results have been obtained mostly for scalar conservation laws. There is a variety of different solution methods for time-dependent partial differential equations. The main classes are spectral methods, finite elements, finite differences and finite volumes. They all have different strengths and drawbacks, and each have several subgroups. In this thesis, we will mostly focus on finite difference methods.

1.4.1 Finite Difference Schemes

These methods are well developed for conservation laws. Typically, in this case, goal is to approximate solutions to differential equations, i.e., to find a function (or some discrete approximation to this function) which satisfies a given relationship between various of its derivatives on some given region of space and/or time, along with some boundary conditions along the edges of this domain. In general this is a difficult problem and only rarely can an analytic formula be found for the solution. A finite difference method proceeds by replacing the derivatives in the differential equations by finite difference approximations. This gives a large algebraic system of equations to be solved in place of the differential equation, something that is easily solved on a computer.

A finite difference method for (1.1.1) is given by,

$$\frac{\Delta u}{\Delta t} + \frac{\Delta f(u)}{\Delta x} = 0. \tag{1.4.1}$$

Here Δt and Δx are small positive numbers. We shall use the notation

$$U_j^n = u(j\Delta x, n\Delta t) \quad \text{and} \quad U^n = (U_{-K}^n, \cdots, U_j^n, \cdots, U_K^n),$$

where U now is our numerical approximation to the solution of (1.1.1). Normally, since we are interested in the initial value problem (1.1.1), we know the initial approximation

$$U_j^0, \quad -K \le j \le K,$$

and we want to use (1.4.1) to calculate U^n for $n \in \mathbb{N}$.
We call a finite difference method **conservative** if it can be written in the form :

$$\begin{aligned} U_j^{n+1} &= G(U_{j-1-p}^n, \cdots, U_{j+q}^n) \\ &= U_j^n - \lambda \left(F(U_{j-p}^n, \cdots, U_{j+q}^n) - F(U_{j-1-p}^n, \cdots, U_{j-1+q}^n) \right), \end{aligned} \tag{1.4.2}$$

where

$$\lambda = \frac{\Delta t}{\Delta x}.$$

The function F is referred to as the **numerical flux.** For brevity, we shall often use the notation

$$G(U; j) = G(U_{j-1-p}, \cdots, U_{j+q}),$$

$$F(U;j) = F(U_{j-p}, \cdots, U_{j+q}),$$

so that (1.4.2) reads

$$U_j^{n+1} = G(U^n;j) = U_j^n - \lambda(F(U^n;j) - F(U^n;j-1)).$$

Conservative methods have the property that U is conserved, since

$$\sum_{j=-K}^{K} U_j^{n+1}\Delta x = \sum_{j=-K}^{K} U_j^n \Delta x - \Delta t(F(U^n;K) - F(U^n;-K-1)).$$

If we set U_j^0 equal to the average of u_0 over the j-th grid cell, i.e.,

$$U_j^0 = \frac{1}{\Delta x}\int_{j\Delta x}^{(j+1)\Delta x} u_0(x)\,dx,$$

and for the moment assume that $F(U^n;K) = F(U^n;-K-1)$, then

$$\int U^n(x)\,dx = \int u_0(x)\,dx.$$

A conservative method is said to be **consistent** if

$$F(u, \cdots, u) = f(u).$$

Definition 1.4.1. *(CFL-condition): A numerical method can be convergent only if its numerical domain of dependence contains the true domain of dependence of the PDE, at least in the limit as Δt, Δx go to zero.*

For finite difference schemes we have typically the following restriction on the size of the time step

$$\max_i |\lambda_i^n| \frac{\Delta t^n}{\Delta x} \leq c,$$

where λ_i^n is the largest eigenvalue of the flux f, and the constant c is the CFL-number of the numerical method.

The following theorem states the importance of the method being based on the conservative form, see [25].

Theorem 1.4.1. *(Lax-Wendroff theorem) Consider a sequence of grids indexed by $j = 1, 2, ...$ with mesh parameters $\Delta t^{(j)}, \Delta x^{(j)} \to 0$ as $j \to \infty$. Let $Q^{(j)}(x,t)$ denote the numerical approximation computed with a consistent and conservative method on the j-th grid. Suppose that $Q^{(j)}$ converges to a function q as $j \to \infty$, i.e.,*

$$\left\|Q^{(j)} - q\right\|_p \to 0, as \quad j \to \infty,$$

where $\|.\|_p$. is the usual norm in L^p. Then $q(x,t)$ is a weak solution of the conservation law.

The **local truncation error** of a numerical method $L_{\Delta t}$ is defined (formally) as

$$L_{\Delta t}(x) = \frac{1}{\Delta t}(S(\Delta t)u - S_N(\Delta t)u)(x),$$

where $S(t)$ is the solution operator associated with (1.1.1); that is, $u = S(t)u_0$ denotes the solution at time t, and $S_N(t)$ is the formal solution operator associated with the numerical method, i.e.,

$$S_N(\Delta t)u(x) = u(x) - \lambda(F(u; j) - F(u; j-1)).$$

We say that the method is of k-th order if for all smooth solutions $u(x, t)$,

$$|L_{\Delta t}(x)| = \mathcal{O}(\Delta t^k)$$

as $\Delta t \to 0$. That a method is of high order, $k \geq 2$, usually implies that it is "good" for computing smooth solutions.

1.4.2 Boundary conditions

Roughly speaking, boundary conditions are the set of conditions specified for the behavior of the solution to a set of differential equations at the boundary of its domain. Boundary conditions are important in determining the mathematical solutions to many physical problems. In a numerical simulation, it is impossible and unnecessary to simulate the whole universe. Generally we choose a region of interest in which we conduct a simulation. The interesting region has a certain boundary with the surrounding environment. Numerical simulations also have to consider the physical processes in the boundary region. In most cases, the boundary conditions are very important for the simulation region's physical processes. Different boundary conditions may cause quite different simulation results. Improper sets of boundary conditions may introduce non-physical influences on the simulation system, while a proper set of boundary conditions can avoid that. So arranging the boundary conditions for different problems becomes very important. While at the same time, different variables in the environment may have different boundary conditions according to certain physical problems.

Commonly there are several different types of boundary conditions:

- **Dirichlet boundary condition:** The Dirichlet boundary condition is a type of boundary condition, named after Johann Peter Gustav Lejeune Dirichlet. When imposed on a partial differential equation, it specifies the values a solution needs to take on the boundary of the domain. The question of finding solutions to such equations is known as the Dirichlet problem. For a partial differential equation on a domain Ω such as

$$\Delta u + u = 0,$$

the Dirichlet boundary condition takes the form:

$$u(x) = f(x), \quad \forall x \in \partial\Omega.$$

- **Neumann boundary condition:** The Neumann boundary condition is a type of boundary condition, named after Carl Neumann. When imposed on an ordinary or a

partial differential equation, it specifies the values that the derivative of a solution is to take on the boundary of the domain. For a partial differential equation on a domain Ω such as

$$\Delta u = 0,$$

the Neumann boundary condition takes the form:

$$\nabla u(x).\mathbf{n}(x) = f(x), \quad \forall x \in \partial\Omega,$$

where, $\mathbf{n}$ denotes the (typically exterior) normal to the boundary $\partial\Omega$.

- **Mixed boundary condition:** A mixed boundary condition for a partial differential equation indicates that different boundary conditions are used on different parts of the boundary of the domain of the equation. For example, if u is a solution to a partial differential equation on a set Ω with piecewise-smooth boundary $\partial\Omega$, and $\partial\Omega$ is divided into two parts Γ_1 and Γ_2, one can use a Dirichlet boundary condition on Γ_1 and a Neumann boundary condition on Γ_2:

$$u \mid_{\Gamma} = v_0, \quad \frac{\partial u}{\partial \mathbf{n}} = v_1,$$

where v_0 and v_1 are given functions defined on those portions of the boundary.

1.4.3 Summation-by-parts schemes

In general, finite difference schemes are relatively easy to code, and such schemes utilise computers efficiently. The summation-by-parts (SBP) finite difference schemes for one-dimensional derivative approximations are as follows: Let $[0, 1]$ be the domain discretized with $x_j = j\Delta x$, $j = 0, 1, \cdots, N-1$. A scalar grid function is defined as $w = (w_0, w_1, \cdots, w_{N-1})$. To approximate w_x we use a SBP operator $D = P^{-1}Q$, where P and Q have the following properties:

$$P = P^T, \quad x^T P x > 0 \quad \text{for all } x,$$
$$Q + Q^T = B = \text{diag}(-1, 0, \cdots, 0, 1).$$

Also P is used to define an inner product $(v, w)_P = v^T P w$, such that the associated norm $\|w\|_P = (w, w)_P^{1/2}$ is equivalent to the norm $\|w\| = (\Delta x \sum_k w_k^2)^{1/2}$. In the work by Kreiss and Scherer [29, 30], which was followed by Strand [31, 1] high-order finite difference operators with a summation-by-parts (SBP) property were derived for first derivative approximations. Stability for these schemes can easily be proven with energy estimates for equations in one space dimension.

Implementing boundary conditions in a stable manner always makes the stability analysis rather difficult. Also we know that a high-order finite difference scheme resolves the solution much better but the analysis of boundary conditions becomes complicated and it is not trivial to implement boundary conditions in a stable manner. Naive ways of implementing boundary conditions often result in stable schemes, and theoretically it is possible to analyse the effect on stability from the boundary conditions. However, the accuracy is often not satisfying.

Carpenter et al. [28] introduced a new way to implement boundary condi- tions weakly for finite difference methods, with the Simultaneous Approximation Term (SAT) technique. The technique involves penalty terms which make energy estimates for PDEs in several space dimensions possible. In a series of articles by Nordström and Carpenter [26, 27] this technique was developed for SBP operators and they also use this technique to patch grids together, proving stability and conservation for such interfaces. The patching of different grids allows the finite difference technique to be used for problems with more complex geometries.

Below, we shall derive the energy estimates for both advection and advection-diffusion equations.

• **Continuous and Discrete energy estimates for advection equation:** Consider the equation

$$\begin{aligned} u_t + u_x &= 0, \quad 0 \le t \le 1, \quad 0 \le x \le 1 \\ u(x,0) &= f(x), \\ u(0,t) &= g(t). \end{aligned} \tag{1.4.3}$$

To derive a bound on u, we will multiply (1.4.3) by u and integrate in space, yields

$$(\int_0^1 u^2\,dx)_t + u(1,t)^2 = g(t)^2. \tag{1.4.4}$$

By denoting $\|u\|^2 = \int_0^1 u^2\,dx$, (1.4.4) gives

$$\|u\|^2 + \int_0^T u(1,t)^2\,dt = \|f\|^2 + \int_0^T g(t)^2\,dt.$$

i.e., u is bounded.

Now in the discrete case, let us define the approximation solution $v = (v_0, v_1, \cdots, v_N)^T$ on the grid. Now an semi-discrete SBP-SAT discretization of (1.4.3) is,

$$v_t + Dv = \sigma P^{-1} e_0 (v_0 - g), \tag{1.4.5}$$

where σ is a parameter to be determind and $e_0 = (1, 0, \cdots, 0)^T$. The analogous derivation of the continuous energy estimate is given by the following. First muliplying (1.4.5) by $v^T P$ results,

$$v^T P v_t + v^T Q v = \sigma v^T e_0 (v_0 - g),$$

which implies,

$$(\|v\|_P^2)_t + v^T (Q + Q^T) v = 2\sigma v^T e_0 (v_0 - g),$$

consequently, we end up with

$$(\|v\|_P^2)_t - v_0^2 + v_N^2 = 2\sigma(v_0^2 - v_0 g).$$

Stability (that is v bounded, with $g = 0$) is achieved for $\sigma \le -1/2$. With $\sigma = -1$ we have,

$$(\|v\|_P^2)_t + v_N^2 = g^2 - (v_0 - g)^2.$$

i.e., the same estimate (with an additional small dissipative term) is obtained as in the continuous case (1.4.4).

• **Continuous and Discrete energy estimates for advection-diffusion equation:** Consider the equation

$$\begin{aligned} u_t + au_x &= \epsilon u_{xx}, \quad 0 \le x \le 1, \quad t \ge 0 \\ u(x,0) &= f(x), \\ u(0,t) &= 0, \quad au(1,t) - 2\epsilon u_x(1,t) = 0 \end{aligned} \tag{1.4.6}$$

where $a, \epsilon > 0$. The boundary at $x = 0$ is a model of wall (and the $x = 1$ mimics a far-field boundary condition). The energy method gives,

$$\begin{aligned} \frac{1}{2}\left(\int_0^1 u^2\,dx\right)_t + \frac{au(1,t)^2}{2} - \frac{au(0,t)^2}{2} \\ = \epsilon u(1)u_x(1) - \epsilon u(0)u_x(0) - \epsilon\int_0^1 u_x^2\,dx. \end{aligned}$$

Using the boundary condition yields,

$$\frac{1}{2}\left(\int_0^1 u^2\,dx\right)_t + \epsilon\int_0^1 u_x^2\,dx = 0.$$

Hence, $\|u\|$ is bounded.

A SBP-SAT semi-discrete approximation to (1.4.6) is given by

$$\begin{aligned} &v_t + aP^{-1}Qv \\ &= \epsilon P^{-1}QP^{-1}Qv + \sigma_L E_0 P^{-1}(v - g_L) + \sigma_R E_1 P^{-1}(av - 2\epsilon P^{-1}Qv - g_R), \end{aligned}$$

where σ_L and σ_R are parameters to be determined with respect to stability, also $E_0 = \mathrm{diag}(1, 0, \cdots, 0)$ and $E_1 = \mathrm{diag}(0, \cdots, 0, 1)$. With $g_L = g_R = 0$, we apply the energy method by multiplying by $v^T P$ and adding the result to its transpose

$$\begin{aligned} (\|v\|_P^2)_t + av^T Bv = 2\epsilon v^T BP^{-1}Qv - 2\epsilon(P^{-1}Qv)^T P(P^{-1}Qv) \\ + 2\sigma_L v^T E_0 v + 2\sigma_R v^T E_1(av - 2\epsilon P^{-1}Qv). \end{aligned}$$

With $\sigma_R = 1/2$, all boundary terms at $x = 1$ cancel and the right boundary is stable. We will use the short notation $v_{xi} = (P^{-1}Qv)_i$ and assume that P is diagonal with upper-left component hp_0. (Note that $p_0 > 0$.) Then

$$(\|v\|_P^2)_t - av_0^2 = -2\epsilon v_0 v_{x0} - 2\epsilon v_x^T P v_x + 2\sigma_L v_0^2. \tag{1.4.7}$$

The aim is to choose σ_L such that $\|v\|$ becomes non-increasing. To achieve that, we would like to rewrite the boundary terms as a quadratic form. Since no boundary term with v_{x0}^2 appears explicitely, it seems to be an impossible task. However, we may use

$$v_x^T P v_x = v_{x0}^2 hp_0 + h\sum_{i=1}^{N} v_{xi}^2 p_i = v_{x0}^2 hp_0 + \|v_x\|_{\mathcal{P}}^2.$$

Then (1.4.7) becomes

$$(\|v\|_P^2)_t + 2\epsilon \|v_x\|_{\mathcal{P}}^2 + r^T M r = 0,$$

where $r^T = (v_0, v_{x0})$ and

$$M = \begin{pmatrix} -2\sigma_L - a & \epsilon \\ \epsilon & 2\epsilon h p_0 \end{pmatrix}.$$

If M is positive semidefinite, then the scheme is stable. Introduce, $\sigma_L = \sigma_1 + \epsilon\sigma_2$ and split M such that

$$M = M_1 + \epsilon M_2 = \begin{pmatrix} -2\sigma_1 - a & 0 \\ 0 & 0 \end{pmatrix} + \epsilon \begin{pmatrix} -2\sigma_2 & 1 \\ 1 & 2hp_0 \end{pmatrix}.$$

M is positive semidefinite, if M_1 and M_2 are. M_1 is positive semidefinite if $\sigma_1 \leq -a/2$ and M_2 if $\sigma_2 \leq -\frac{1}{4hp_0}$.

1.5 Magnetic Induction Equations

The magnetic induction equations are a special form of the Maxwell's equations which describes the evolution of the magnetic field under the influence of a given velocity field. These equations arise in a wide variety of applications in plasma physics, astrophysics and electrical engineering. One important application are the equations of magneto-hydro dynamics (MHD), see [2] for details. These equations combine the Euler equations of gas dynamics with the magnetic induction equations, leading to the following semi-conservative form of the ideal MHD equations with divergence constraint,

$$\begin{aligned}
\rho_t + \operatorname{div}(\rho \mathbf{u}) &= 0, \\
(\rho \mathbf{u})_t + \operatorname{div}\left(\rho \mathbf{u} \otimes \mathbf{u} + \left(p + \frac{1}{2}\mathbf{B}^2\right)\mathcal{I} - \mathbf{B} \otimes \mathbf{B}\right) &= 0, \\
E_t + \operatorname{div}\left(\left(E + p + \frac{1}{2}\mathbf{B}^2\right)\mathbf{u} - (\mathbf{u} \cdot \mathbf{B})\,\mathbf{B}\right) &= 0, \\
\mathbf{B}_t + \operatorname{div}\left(\mathbf{u} \otimes \mathbf{B} - \mathbf{B} \otimes \mathbf{u}\right) &= 0, \\
\operatorname{div}\mathbf{B} &= 0,
\end{aligned}$$

together with equation of state

$$E = \frac{p}{\gamma - 1} + \frac{1}{2}\rho|\mathbf{u}|^2 + \frac{1}{2}|\mathbf{B}|^2.$$

In the above model, the variables of interest are the mass density of the plasma ρ, the velocity field $\mathbf{u} = (u^1, u^2, u^3)^T$, the magnetic field $\mathbf{B} = (B^1, B^2, B^3)^T$, the pressure p, and the total energy E.

In case of magnetic induction equations, the variables of interest are the velocity field $\mathbf{u} = (u^1, u^2, u^3)^T$ (known) and the magnetic field $\mathbf{B} = (B^1, B^2, B^3)^T$ (unknown). The unknown follows certain balance laws.

1.5.1 Derivation of the Magnetic Induction equations

The derivation of the Magnetic Induction equations in three spacial dimensions is described below.

Faraday's law: The magnetic flux across a surface $\mathbf{S}$ bounded by a curve $\partial\mathbf{S}$ is given by, see [7]

$$-\frac{d}{dt}\int_S \mathbf{B}\cdot\mathbf{dS} = \oint_{\partial S}\mathbf{E}'\cdot dl.$$

Using the Stokes theorem and the fact that the electric field, $\mathbf{E}'$, in a co-moving frame is zero, Faraday's law takes the form,

$$\partial_t\mathbf{B} + \mathrm{curl}(\mathbf{B}\times\mathbf{u}) = -\mathbf{u}\mathrm{div}(\mathbf{B}). \tag{1.5.1}$$

The above equation is called the magnetic induction equations and using simple vector identites, (1.5.1) can be rewritten as,

$$\frac{\partial\mathbf{B}}{\partial t} + \mathrm{div}(\mathbf{u}\otimes\mathbf{B} - \mathbf{B}\otimes\mathbf{u}) = -\mathbf{u}\mathrm{div}(\mathbf{B}). \tag{1.5.2}$$

The above form is also called the **Godunov-Powell form** of the magnetic induction equations, and the source on the right-hand side of (1.5.2) is called the **Godunov-Powell source term.**

Magnetic monopoles have never been observed in nature, although their existence has been hypothesized in a number of quantum regimes by both the unified field theory and the string theory. Nevertheless, it is common to assume that the magnetic field is solenoidal, i.e., it satisfies the divergence constraint $\mathrm{div}(\mathbf{B}) = 0$. Hence, it is common to set the right hand side of (1.5.1) to zero and couple the induction equation with the divergence constraint in order to obtain

$$\begin{aligned}\partial_t\mathbf{B} + \mathrm{curl}(\mathbf{B}\times\mathbf{u}) &= 0,\\ \mathrm{div}(\mathbf{B}) &= 0.\end{aligned} \tag{1.5.3}$$

This form (1.5.3) is commonly used in the literature as the appropriate form of the magnetic induction equations to study and discretize. It is easy to see that (1.5.3) is hyperbolic but not strictly hyperbolic. An important tool in the analysis of hyperbolic system of equations is the derivation of energy estimates. The usual procedure in deriving energy estimates consists of symmetrizing the hyperbolic system. It is not possible to symmetrize (1.5.3) without explicitly using the divergence constraint. Hence, it is difficult to obtain energy stability starting from (1.5.3).

On the other hand, we can use the following vector identity

$$\begin{aligned}\mathrm{curl}(\mathbf{B}\times\mathbf{u}) &= \mathbf{B}\mathrm{div}\mathbf{u} - \mathbf{u}\mathrm{div}(\mathbf{B}) + (\mathbf{u}\cdot\nabla)\,\mathbf{B} - (\mathbf{B}\cdot\nabla)\,\mathbf{u}\\ &= \left(u^1\mathbf{B}\right)_x + \left(u^2\mathbf{B}\right)_y + \left(u^3\mathbf{B}\right)_z - \mathbf{u}\mathrm{div}(\mathbf{B}) - (\mathbf{B}\cdot\nabla)\mathbf{u},\end{aligned}$$

and rewrite (1.5.2) in the non-conservative symmetric form,

$$\begin{aligned}\partial_t\mathbf{B} + (\mathbf{u}\cdot\nabla)\,\mathbf{B} &= -\mathbf{B}(\mathrm{div}\mathbf{u}) + (\mathbf{B}\cdot\nabla)\mathbf{u}\\ &= M(D\mathbf{u})\mathbf{B},\end{aligned} \tag{1.5.4}$$

where the matrix $M(D\mathbf{u})$ is given by

$$M(D\mathbf{u}) = \begin{pmatrix} -\partial_y u^2 - \partial_z u^3 & \partial_y u^1 & \partial_z u^1 \\ \partial_x u^2 & -\partial_x u^1 - \partial_z u^3 & +\partial_z u^2 \\ \partial_x u^3 & \partial_y u^3 & -\partial_x u^1 - \partial_y u^2 \end{pmatrix}.$$

Introducing the matrix,

$$C = -\begin{pmatrix} \partial_x u^1 & \partial_y u^1 & \partial_z u^1 \\ \partial_x u^2 & \partial_y u^2 & \partial_z u^2 \\ \partial_x u^3 & \partial_y u^3 & \partial_z u^1 \end{pmatrix},$$

(1.5.2) can also be written in the following "conservative" symmetric form,

$$\partial_t \mathbf{B} + \partial_x \left(A^1 \mathbf{B}\right) + \partial_y \left(A^2 \mathbf{B}\right) + \partial_z \left(A^3 \mathbf{B}\right) + C\mathbf{B} = 0, \tag{1.5.5}$$

where $A^i = u^i I$ for $i = 1, 2, 3$. Note that the symmetrized matrices in (1.5.5) are diagonal and that the only coupling in the equations is through the lower order source terms. These symmetrized forms are in the same spirit as the non-linear symmetrized forms of MHD equations introduced in [8].

Furthermore, by taking divergence on both sides of (1.5.1) we get

$$(\mathrm{div}(\mathbf{B}))_t + \mathrm{div}\left(\mathbf{u}\mathrm{div}(\mathbf{B})\right) = 0. \tag{1.5.6}$$

Hence, if $\mathrm{div}(\mathbf{B}_0(\mathbf{x})) = 0$, also $\mathrm{div}(\mathbf{B}(\mathbf{x}, t) = 0$ for $t > 0$. This implies that all the above forms (1.5.5), and (1.5.3) are equivalent (at least for smooth solutions).

1.5.2 Numerical aspects of magnetic induction equations

Even though the magnetic induction equations are linear, the presence of variable coefficients and lower order terms means that general closed form solutions are not available. Hence, one has to design suitable numerical schemes for these equations. Furthermore, since these equations appear as a sub-model in the MHD equations, the design of stable and high-order accurate numerical schemes for the induction equations can lead to the design of robust schemes for the non-linear MHD equations.

Most of the attention in the literature has been focused on the constrained form (1.5.3). The key issue in the design of a suitable numerical scheme to approximate (1.5.3) has been the treatment of the divergence constraint. A widely used approach has been to employ projection methods based on a Hodge decomposition of the magnetic field. A base (finite difference or finite volume) scheme is used to evolve the magnetic field. The evolved field, which may not be divergence free, is then corrected for divergence errors by solving an elliptic equation (see [4]). The resulting method is computationally expensive, as the elliptic equation has to be solved at every time step.

Another common approach is to discretize (1.5.3) such that some particular form of discrete divergence is preserved at each time step (see [11]). This approach is equivalent to staggering the velocity and magnetic fields in each direction (see [4, 1, 20, 5] and a detailed comparison in [12]). Some of these schemes are proved to be von Neumann stable in the special case of constant velocity fields. No stability analysis is available either in the

case of variable velocity fields or for problems with boundary conditions. These schemes also involve wider stencils than what is required for a standard finite difference scheme.

Despite all the attempts at finding a suitable discretization of (1.5.3) and preserving a special form of discrete divergence, it is not clear whether such an approach is appropriate. Furthermore, there are many different choices for the discrete divergence operator and preserving some form of discrete divergence exactly does not lead to preservation or even to small divergence errors for a different form. The main aim should be to design a stable scheme to approximate magnetic fields, and it is not clear whether preserving divergence in a particular discrete form helps. One reason for the difficulties in proving stability of discretizations for (1.5.3) with general velocity fields may lie in the very form of these equations. As remarked earlier, (1.5.3) are not symmetrizable directly and thus one cannot obtain energy estimates in this form. This remains true for discretizations of (1.5.3).

A different approach consisting of discretizing the physical form (1.5.2) was proposed in [17] for the non-linear MHD equations. Adapting this to (1.5.2) entails using a standard upwind scheme for the convection part and a centered discretization of the source terms. From (1.5.6), one can expect that divergence errors will be transported out of the domain for transparent boundary conditions. This approach does not imply stability either, and can lead to oscillations, as reported in [5]. A discontinuous Galerkin based discretization of the symmetric form (1.5.5) was proposed in [2].

In a recent paper [5], the authors discretized the symmetric form (1.5.4) by using a first order accurate upwind finite difference scheme. The resulting scheme also implied an upwind discretization of the convection term in (1.5.2) with an upwind discretization of the source term. This scheme was shown to be energy stable even with variable velocity fields and to be TVD for constant velocity fields.

1.6 Magnetic induction equations with resistivity

Magnetic induction equations with resistivity is an extension of magnetic induction equations. These equations are a system of convection-diffusion equations with the magnetic resistivity and heat conduction playing the role of diffusion. Many applications like plasma thrusters for deep space propulsion and electromagnetic pulse devices involve small (but non-zero) values of the magnetic resistivity. This is a submodel of MHD equations with resistivity, given by

$$\begin{aligned}
\rho_t + \mathrm{div}(\rho\mathbf{u}) &= 0,\\
(\rho\mathbf{u})_t + \mathrm{div}(\rho\mathbf{u}\otimes\mathbf{u} + (p + \frac{1}{2}|\mathbf{B}|^2)I - \mathbf{B}\otimes\mathbf{B}) &= -\mathbf{B}(\mathrm{div}\mathbf{B}),\\
E_t + \mathrm{div}((E + p + \frac{1}{2}|\mathbf{B}|^2)\mathbf{u} - (\mathbf{u}\cdot\mathbf{B})\mathbf{B}) &= -(\mathbf{u}\cdot\mathbf{B})(\mathrm{div}\mathbf{B}),\\
\mathbf{B}_t + \mathrm{div}(\mathbf{u}\otimes\mathbf{B} - \mathbf{B}\otimes\mathbf{u}) &= -\mathbf{u}(\mathrm{div}\mathbf{B}) - \epsilon\mathrm{curl}(\mathrm{curl}(\mathbf{B}))
\end{aligned}$$

This is called Godunov-Powell form of resistive MHD equations. When the fluid cannot be considered as completely conductive, but the other conditions for ideal MHD are satisfied, it is possible to use an extended model called resistive MHD. Resistive MHD describes magnetized fluids with finite magnetic diffusivity ($\epsilon \neq 0$). This diffusivity leads

to a breaking in the magnetic topology; magnetic field lines can "reconnect" when they collide. Usually this term is small and reconnections can be handled by thinking of them as not dissimilar to shocks; this process has been shown to be important in the Earth-Solar magnetic interactions.

1.6.1 Derivation of Magnetic Induction Equations with Resistivity

In a moving medium, the time rate of change of the magnetic flux across a given surface $\mathbf{S}$ bounded by curve $\partial\mathbf{S}$ is given by [7]:

$$\frac{d}{dt}\int\limits_S \mathbf{B}\cdot\mathbf{dS} = \int\limits_S \frac{\partial\mathbf{B}}{\partial t}\cdot\mathbf{dS} + \oint\limits_{\partial S}\mathbf{B}\times\mathbf{u}\cdot dl + \int\limits_S (\mathrm{div}(\mathbf{B}))\mathbf{u}\cdot\mathbf{dS} + \epsilon\oint\limits_{\partial S}\mathbf{J}\cdot dl,$$

where the unknown $\mathbf{B} = \mathbf{B}(\mathbf{x},t) \in \mathbb{R}^3$ denotes the magnetic field, $\mathbf{J} = \mathbf{J}(\mathbf{x},t) \in \mathbb{R}^3$ the current density and $\mathbf{x} = (x,y,z)$ are the spatial coordinates. The current density is given by: $\mathbf{J} = \mathrm{curl}(\mathbf{B})$. The parameter ϵ denotes the magnetic resistivity, and $\mathbf{u}(\mathbf{x},t)$ the (given) velocity field.

Using Faraday's law:

$$-\frac{d}{dt}\int\limits_S \mathbf{B}\cdot\mathbf{dS} = \oint\limits_{\partial S}\mathbf{E}'\cdot dl, \tag{1.6.1}$$

Stokes' theorem, the fact that the electric field $\mathbf{E}' = 0$ in a co-moving frame and $\mathbf{E}' = \mathbf{E} + \mathbf{u}\times\mathbf{B}$ we obtain,

$$\frac{\partial\mathbf{B}}{\partial t} + \mathrm{curl}(\mathbf{B}\times\mathbf{u}) = -\mathbf{u}\mathrm{div}(\mathbf{B}) - \epsilon\mathrm{curl}(\mathrm{curl}(\mathbf{B})). \tag{1.6.2}$$

Since magnetic monopoles have never been observed in nature, we can assume as before that $\mathrm{div}(\mathbf{B}) = 0$. Using this constraing in (1.6.2), we obtain the system:

$$\begin{aligned} \partial_t\mathbf{B} + \mathrm{curl}(\mathbf{B}\times\mathbf{u}) &= -\epsilon\mathrm{curl}(\mathrm{curl}(\mathbf{B})),\\ \mathrm{div}(\mathbf{B}) &= 0. \end{aligned} \tag{1.6.3}$$

The above equation is an example of a convection-diffusion equation. The version obtained by taking zero resistivity ($\epsilon = 0$) in (1.6.3) is termed the magnetic induction equation ([33]). A standard way to obtain a bound on the solutions of convection-diffusion equations like (1.6.3) is to use the energy method. However (1.6.3) is not symmetrizable. Consequently it may not be possible to obtain an energy estimate for this system.

On the other hand, (1.6.2) is symmetrizable. We use the following vector identity

$$\begin{aligned} \mathrm{curl}(\mathbf{B}\times\mathbf{u}) &= \mathbf{B}\mathrm{div}\mathbf{u} - \mathbf{u}\mathrm{div}(\mathbf{B}) + (\mathbf{u}\cdot\nabla)\,\mathbf{B} - (\mathbf{B}\cdot\nabla)\,\mathbf{u}\\ &= \left(u^1\mathbf{B}\right)_x + \left(u^2\mathbf{B}\right)_y + \left(u^3\mathbf{B}\right)_z - \mathbf{u}\mathrm{div}(\mathbf{B}) - (\mathbf{B}\cdot\nabla)\mathbf{u}, \end{aligned}$$

and rewrite (1.6.2) in the form,

$$\begin{aligned} \partial_t\mathbf{B} + (\mathbf{u}\cdot\nabla)\,\mathbf{B} &= -\mathbf{B}(\mathrm{div}\mathbf{u}) + (\mathbf{B}\cdot\nabla)\mathbf{u} - \epsilon\mathrm{curl}(\mathrm{curl}(\mathbf{B}))\\ &= M(D\mathbf{u})\mathbf{B} - \epsilon\mathrm{curl}(\mathrm{curl}(\mathbf{B})), \end{aligned} \tag{1.6.4}$$

where the matrix $M(D\mathbf{u})$ is given by

$$M(D\mathbf{u}) = \begin{pmatrix} -\partial_y u^2 - \partial_z u^3 & \partial_y u^1 & \partial_z u^1 \\ \partial_x u^2 & -\partial_x u^1 - \partial_z u^3 & \partial_z u^2 \\ \partial_x u^3 & \partial_y u^3 & -\partial_x u^1 - \partial_y u^2 \end{pmatrix}.$$

Introducing the matrix,

$$C = -\begin{pmatrix} \partial_x u^1 & \partial_y u^1 & \partial_z u^1 \\ \partial_x u^2 & \partial_y u^2 & \partial_z u^2 \\ \partial_x u^3 & \partial_y u^3 & \partial_z u^1 \end{pmatrix},$$

(1.6.2) can also be written in the following form,

$$\partial_t \mathbf{B} + \partial_x \left(A^1 \mathbf{B}\right) + \partial_y \left(A^2 \mathbf{B}\right) + \partial_z \left(A^3 \mathbf{B}\right) + C\mathbf{B} = -\epsilon \text{curl}(\text{curl}(\mathbf{B})), \tag{1.6.5}$$

where $A^i = u^i I$ for $i = 1, 2, 3$. Note that the symmetrized matrices in (1.6.5) are diagonal and that the coupling in the equations are through both the lower order source terms and the viscous terms.

Furthermore, taking the divergence of both sides of (1.6.2) we obtain,

$$(\text{div}(\mathbf{B}))_t + \text{div}\left(\mathbf{u}\text{div}(\mathbf{B})\right) = 0. \tag{1.6.6}$$

Hence, if $\text{div}(\mathbf{B}_0(\mathbf{x})) = 0$, it follows that $\text{div}(\mathbf{B}(\mathbf{x}, t)) = 0$ for $t > 0$. This implies that all the above forms (1.6.5), (1.6.3) and (1.6.2) are equivalent (at least for smooth solutions).

1.7 Summary of Paper I

The magnetic induction equations (1.5.1) can be viewed as a simple model equation for MHD where we already know the velocity field. In this paper we design stable and high-order accurate schemes for initial-boundary value problems corresponding to the magnetic induction equations by discretizing the non-conservative symmetric form (1.5.5) (i.e., using the Godunov-Powell source term). The spatial derivatives are approximated by second and fourth-order SBP (Summation-By-Parts) operators. The boundary conditions are weakly imposed by using a SAT (Simultaneous Approximation Term) and time integration is performed by standard Runge-Kutta schemes. We also report several experiments that show that the scheme of this paper is robust.

1.7.1 Numerical experiment

In this experiment, we consider (1.5.1) with the divergence-free velocity field $\mathbf{u}(x, y) = (-y, x)^T$. The exact solution can be easily calculated by the method of characteristics and takes the form

$$\mathbf{B}(\mathbf{x}, t) = R(t)\mathbf{B}_0(R(-t)\mathbf{x}), \tag{1.7.1}$$

where $R(t)$ is a rotation matrix with angle t and represents rotation of the initial data about the origin.

We consider the divergence free initial data,

$$\mathbf{B}_0(x,y) = 4\begin{pmatrix} -y \\ x-\frac{1}{2} \end{pmatrix} e^{-20\left((x-1/2)^2+y^2\right)}, \tag{1.7.2}$$

and the computational domain $[-1,1]\times[-1,1]$. Since the exact solution is known in this case, one can in principle use this to specify the boundary data g. Instead, we decided to mimic a free space boundary (artificial boundary) by taking $g = 0$. (which is a good guess at a far-field boundary).

We run this test case with $SBP2$ and $SBP4$ schemes and present different sets of results. In Figure 1.7.1, we plot $|\mathbf{B}| = (|B^1|^2 + |B^2|^2)^{1/2}$ at times $t = \pi$ (half-rotation) and $t = 2\pi$ (one full rotation) with the $SBP2$ and $SBP4$ schemes. As shown in this

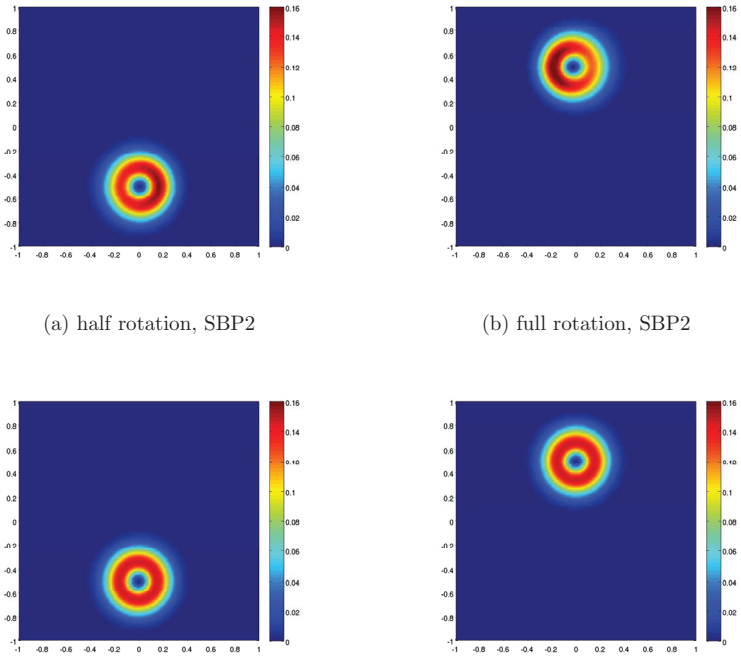

(a) half rotation, SBP2

(b) full rotation, SBP2

(c) half rotation, SBP4

(d) full rotation, SBP4

Figure 1.7.1: Numerical results for $|\mathbf{B}|$.

figure, $SBP2$ and $SBP4$ schemes resolve the solution quite well. In fact, $SBP4$ is very accurate and keeps the hump intact throughout the rotation.

1.8 Summary of Paper II

This paper is an extension of the previous paper. In this paper also, we design stable and high-order accurate schemes for initial-boundary value problems corresponding to the magnetic induction equations with resistivity by discretizing the non-conservative symmetric form (1.6.5) (i.e., using the Godunov-Powell source term). In this paper, we have used two different sets of boundary conditions: Dirichlet and mixed boundary conditions. As in the previous paper, here also the spatial derivatives are approximated by second and fourth-order SBP (Summation-By-Parts) operators. The boundary conditions are weakly imposed by using a SAT (Simultaneous Approximation Term) and time integration is performed by standard Runge-Kutta schemes. Here also we report several experiments that show that the scheme of this paper is robust.

1.8.1 Numerical results

Here we consider a divergence free velocity field $\mathbf{u}(x,y) = (-y,x)^T$ and a slightly modified form of (1.6.5), which in two dimensions is given by

$$\mathbf{B}_t + \Lambda_1 \mathbf{B}_x + \Lambda_2 \mathbf{B}_y - C\mathbf{B} = \epsilon \begin{bmatrix} -((B^2)_{xy} - (B^1)_{yy}) \\ ((B^2)_{xx} - (B^1)_{xy}) \end{bmatrix} + \mathcal{F}, \tag{1.8.1}$$

where the forcing function $\mathcal{F}$ is given by,

$$\begin{aligned} f_1 &= 160\epsilon(y - 0.5\sin(t)) \left[-4 + 40\{(x - 0.5\cos(t))^2 + (y - 0.5\sin(t))^2\}\right] e^{A(t)}, \\ f_2 &= -160\epsilon(y - 0.5\cos(t)) \left[-4 + 40\{(x - 0.5\cos(t))^2 + (y - 0.5\sin(t))^2\}\right] e^{A(t)}, \end{aligned} \tag{1.8.2}$$

with A:

$$A(t) = -20\{(x\cos(t) + y\sin(t) - 0.5)^2 + (-x\sin(t) + y\cos(t))^2\}.$$

It is straightforward to extend the stability results to SBP-SAT schemes for (1.8.1). The forcing term is evaluated in a standard manner. The forcing function in (1.8.1) enables us to calculate an exact (smooth) solution of the equation given by,

$$\mathbf{B}(\mathbf{x},t) = R(t)\mathbf{B}_0(R(-t)\mathbf{x}), \tag{1.8.3}$$

where $R(t)$ is a rotation matrix with angle t.

For initial data, we choose the divergence free magnetic field:

$$\mathbf{B}_0(x,y) = 4 \begin{pmatrix} -y \\ x - \frac{1}{2} \end{pmatrix} e^{-20\left((x-1/2)^2+y^2\right)}, \tag{1.8.4}$$

and the computational domain $[-1,1] \times [-1,1]$. Since the exact solution is known in this case, we use this solution to specify the data for the boundary conditions. Using Dirichlet or mixed boundary conditions led to very similar results. The time-integration was performed with a second-order Runge-Kutta method at a CFL number of 0.5. The resistivity $\epsilon = 0.01$ was used.

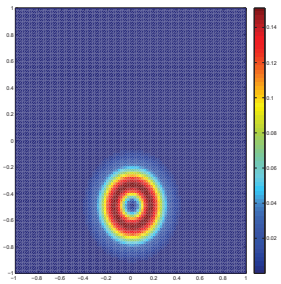

(a) SBP2, half rotation

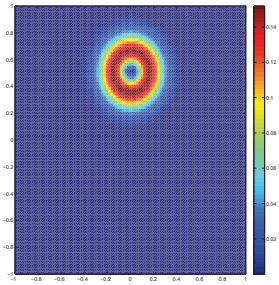

(b) SBP2, full rotation

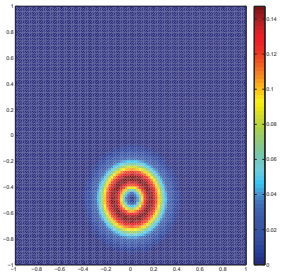

(c) SBP4, half rotation

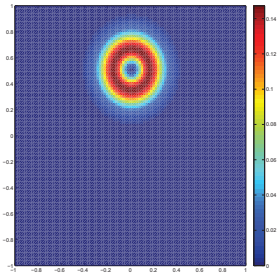

(d) SBP4, full rotation

Figure 1.8.1: Numerical results for $|\mathbf{B}|$.

We plot the l^2 norm of the magnetic field: $\mathbf{B} = \sqrt{(B^1)^2 + (B^2)^2}$, at times $t = \pi$ (half rotation) and $t = 2\pi$ (full rotation) for both the SBP2 and SBP4 schemes in figure 1.8.1. As shown in the figure, both $SBP2$ and $SBP4$ schemes resolve the solution quite well. There are very few noticeable differences between the second and fourth order schemes at this resolution. The shape of the hump is maintained during the rotation.

1.9 Summary of Paper III

This paper is concerned with the initial-boundary value problem of the Kawahara equation:

$$u_t = -uu_x - u_{xxx} + u_{xxxxx}, \tag{1.9.1}$$

with initial condition

$$u(x, 0) = f(x), \quad \text{for all } x \tag{1.9.2}$$

and the boundary condition

$$u(x, t) = u(x + 1, t), \quad \text{for all } x \text{ and } t \tag{1.9.3}$$

It is well known that the one-dimensional waves of small but finite amplitude in dispersive systems (e.g., the magneto-acoustic waves in plasmas, the shallow water waves, the lattice waves and so on) can be described by the Korteweg-de Vries (KdV in short) equation, given by

$$u_t = -uu_x - u_{xxx}, \tag{1.9.4}$$

which admits either compressive or rarefactive steady solitary wave solution (by a solitary water wave, we mean a travelling wave solution of the water wave equations for which the free surface approaches a constant height as $|x| \to \infty$) according to the sign of the dispersion term (the third order derivative term). Under certain circumstances, however, it might happen that the coefficient of the third order derivative in the KdV equation becomes small or even zero. In that case one has to take account of the higher order effect of dispersion in order to balance the nonlinear effect. In such cases one may obtain a generalized nonlinear dispersive equation, known as Kawahara equation, which has a form of the KdV equation with an additional fifth order derivative term given by (1.9.1).

In this paper, we consider both the semi-discrete as well as fully-discrete schemes for the initial-boundary value problem corresponding to (1.9.1). We have showed the convergence of both schemes. Also both the local and global existence of solutions has been proved.

1.9.1 Semi-discrete case

We consider the following semi-discrete scheme of the Kawahara equation (1.9.1), given by

$$(u_i)_t = -\frac{1}{3}[u_i D_0 u_i + D_0 u_i^2] - D_- D_+^2 u_i + D_+^3 D_-^2 u_i, \quad i = 1, 2, ..., N, \tag{1.9.5}$$

with the initial condition

$$u_i(0) = f(x_i), \quad i = 1, 2, ..., N \tag{1.9.6}$$

and the boundary condition

$$u_i(t) = u_{i+N}(t) \quad \text{for all } i \text{ and } t, \tag{1.9.7}$$

where we have used the following finite difference operators:

$$D_- u_i = \frac{1}{\Delta x}(u_i - u_{i-1}), \quad D_+ u_i = \frac{1}{\Delta x}(u_{i+1} - u_i), \quad D_0 u_i = \frac{1}{2\Delta x}(u_{i+1} - u_{i-1}).$$

Later on we will also use the following notations:

$$\|f\|^2 = (f, f) \quad \text{and} \quad (f, g) = \int_0^1 \overline{f(x)} g(x)\, dx,$$

and in the space of gridfunctions (a discrete, possibly complex valued, function defined on the grid), we define the scalar product and the norm by

$$(f, g)_h = h \sum_i \overline{f(x_i)} g(x_i) \quad \text{and } \|f\|_h^2 = (f, f)_h.$$

Local existence of solutions to (1.9.1) follows from the following theorem:

Theorem 1.9.1. *There exists a time $T_1 > 0$ and constants k_i, $i = 0, 1, 2, 3, 4$ independent of Δx but dependent on $f(x)$ and its derivatives of order five and lower, such that*

$$\|u(\cdot, t)\|_h \le k_0, \qquad \textit{for all } t \tag{1.9.8}$$

$$|u(x_i, t)| \le k_1, \qquad 0 \le t \le T_1, \qquad \textit{for all } i \tag{1.9.9}$$

$$\left\|D_- D_+^2 u(\cdot, t)\right\|_h \le k_2, \qquad 0 \le t \le T_1 \tag{1.9.10}$$

$$\left\|D_+^3 D_-^2 u(\cdot, t)\right\|_h \le k_3, \qquad 0 \le t \le T_1 \tag{1.9.11}$$

and finally with,

$$v(x, t) = \frac{\partial u(x, t)}{\partial t}$$

$$\|v(\cdot, t)\|_h \le k_4, \qquad 0 \le t \le T_1. \tag{1.9.12}$$

Proof. (Sketch only) First of all multiplying (1.9.5) by $\Delta x u_i$ and summing over all i (energy method) gives the estimate (1.9.8), where we have used the following two identities:

- $(u, D_- D_+^2 u)_h = \frac{\Delta x}{2} \|D_+ D_- u\|_h^2$.
- $(u, D_+^3 D_-^2 u)_h = -\frac{\Delta x}{2} \left\|D_- D_+^2 u\right\|_h^2$.

On the other hand, from the equation (1.9.5) using the triangle inequality, we can prove the following inequality:

$$\left\|D_+^3 D_-^2 u\right\|_h \leq \nu_1 \|v\|_h + \nu_2, \tag{1.9.13}$$

where $v = u_t$, ν_1 and ν_2 are constants independent of Δx. Now to obtain a bound for $\|v\|_h$, we shall differentiate equation (1.9.5) and use energy method as before. These bounds together with some interpolation inequalities gives all the required estimates stated in the above theorem. Finally, using these bounds, it is quite easy (using Fourier transforms and Arzela-Ascoli theorem) to show the convergence of the semi-discrete scheme. □

On the other hand **global existence** of solutions can be proved using the following two lemmas:

Lemma 1.9.1. *Let $u(x,t)$ be a solution of the problem* (1.9.1)*. Then there exist constants α_1, α_2 such that*

$$\int_0^1 u^2(x,t)\,dx = \int_0^1 u^2(x,0)\,dx = \int_0^1 f^2\,dx = \alpha_1 \tag{1.9.14}$$

$$\int_0^1 \left(\frac{1}{3}u^3 - u_x^2 - u_{xx}^2\right) dx = \int_0^1 \left(\frac{1}{3}f^3 - f'^2 - f''^2\right) dx = \alpha_2 \tag{1.9.15}$$

Lemma 1.9.2. *Let $u(x,t)$ be a solution of the problem* (4.1.1)*. Then there exists a constant α such that*

$$\max|u_x(x,t)| \leq \alpha \tag{1.9.16}$$

$$\|v\|^2 \leq e^{\gamma t}\left\|-ff' - f''' + f''''\right\|^2, \qquad v = \frac{\partial u}{\partial t}. \tag{1.9.17}$$

1.9.2 Fully-discrete case

We propose the following semi-implicit fully-discrete aproximation to (1.9.1), given by

$$\begin{aligned} u_j^{n+1} = \bar{u}_j^n - \frac{\Delta t}{3}[\bar{u}_j^n D_0 u_j^n + D_0(u_j^n)^2] - \Delta t D_- D_+^2 u_j^{n+1} + \Delta t D_+^3 D_-^2 u_j^{n+1}, \\ \text{where} \quad \bar{u}_j = \frac{1}{2}(u_{j+1} + u_{j-1}). \end{aligned} \tag{1.9.18}$$

Now keeping in mind that $D_0 u_j^2 = 2\bar{u}_j D_0 u_j$, we can rewrite the above scheme as

$$u_j^{n+1} = \bar{u}_j^n - \Delta t \bar{u}_j^n D_0 u_j^n - \Delta t D_- D_+^2 u_j^{n+1} + \Delta t D_+^3 D_-^2 u_j^{n+1}. \tag{1.9.19}$$

with the initial condition

$$u_i^0 = f(x_i), \quad i = 1, 2, ..., N, \tag{1.9.20}$$

and the boundary condition

$$u_i^n = u_{i+N}^n \quad \text{for all } i \text{ and } n. \tag{1.9.21}$$

Below we will state the main theorem in the fully discrete case:

Theorem 1.9.2. *There exists a time $T > 0$ and constants k_i, $i = 0, 1, 2, 3, 4$ independent of Δx but dependent on $f(x)$ and its derivatives of order five and lower, such that*

$$\|u^n\|_h \leq k_0, \qquad 0 \leq n\Delta t \leq T \tag{1.9.22}$$

$$|u^n(x_i)| \leq k_1, \qquad 0 \leq n\Delta t \leq T \tag{1.9.23}$$

$$\left\|D_- D_+^2 u^n\right\|_h \leq k_2, \quad 0 \leq n\Delta t \leq T \tag{1.9.24}$$

$$\left\|D_+^3 D_-^2 u^n\right\|_h \leq k_3, \quad 0 \leq n\Delta t \leq T \tag{1.9.25}$$

and finally with,

$$v^n = D_t^+ u^{n-1}, \quad n \in \mathbb{N}_0$$

$$\|v^n\|_h \leq k_4, \quad 0 \leq n\Delta t \leq T. \tag{1.9.26}$$

To prove the above theorem, we have used the similar arguments to the ones used in the semi discrete case.

1.9.3 Summary of numerical results

We have considered the following initial function given by

$$u(x,0) = \frac{105}{169}\text{sech}^4\left(\frac{1}{2\sqrt{13}}(x-c)\right),$$

then it is known that the explicit solution is given by the following travelling wave

$$u(x,t) = \frac{105}{169}\text{sech}^4\left(\frac{1}{2\sqrt{13}}(x-\frac{36t}{169}-c)\right)$$

Since we know that the behaviour of the exact solution for Kawahara equation, mainly which remains its shape as time grows, it will be interesting to see how the numerical solution given by the scheme (1.9.19) evolves with time. We will use the following notations: UK scheme - scheme described in this paper and JMO scheme - scheme described as in [14] and $\|u\|_{l^2} = (\Delta x \sum_k u_k^2)^{\frac{1}{2}}$. In order to compare with the existing scheme given by [14], we present the l^2 errors on a computational domain $[-40, 40]$, between exact solution and the solution generated by the UK and JMO schemes in table 1.9.1.

In the following figures 1.9.1, we show the behaviour of the numerical solutions at different times. In this case we have used a domain $[-20, 50]$, 5000 mesh points and a CFL number 0.75. We will compare our results with the results given by [14].

Mesh points	UK	JMO
4000	2.7e-3	1.2e-3
8000	1.4e-3	6.2e-4
12000	9.2e-4	4.2e-4
16000	7.0e-4	3.0e-4

Table 1.9.1: Numerical Experiment 1: l^2 errors between exact and simulated solutions at time $t = 10$ for both UK and JMO schemes .

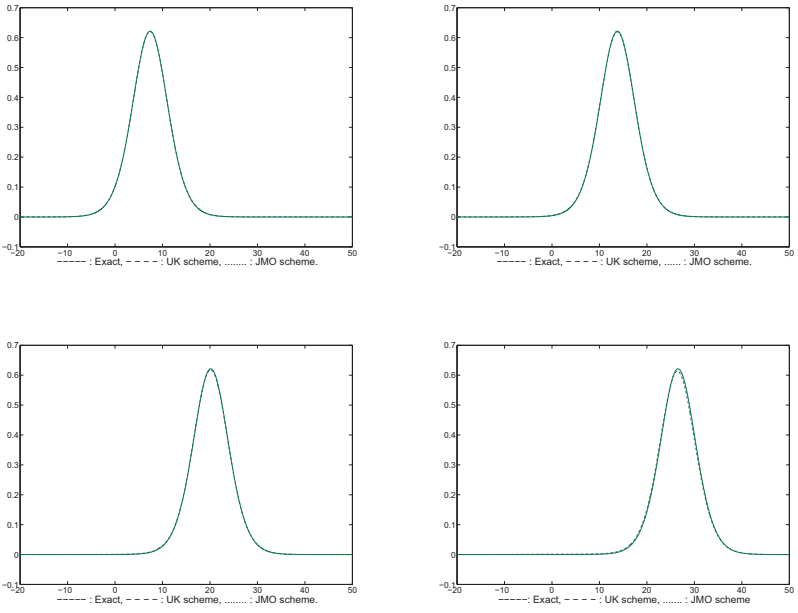

Figure 1.9.1: Top Left: Exact and Numerical solution at time $t = 30$ for both UK scheme and JMO scheme; Top Right: Exact and Numerical solution at time $t = 60$ for both UK scheme and JMO scheme; Bottom Left: Exact and Numerical solution at time $t = 90$ for both UK scheme and JMO scheme; Bottom Right: Exact and Numerical solution at time $t = 120$ for both UK scheme and JMO scheme.

1.10 Summary of Paper IV

In this paper, we consider semi-discrete finite difference schemes for the following Cauchy problem

$$\begin{cases} u_t + f(u)_x = A(u)_{xx}, & (x,t) \in \Pi_T, \\ u(0,x) = u_0(x), & x \in \mathbb{R}, \end{cases} \tag{1.10.1}$$

where $\Pi_T = \mathbb{R} \times (0,T)$ with $T > 0$ fixed, $u : \Pi_T \to \mathbb{R}$ is the unknown function, f the flux function, and A the nonlinear diffusion. Regarding this, the basic assumption is that $A' \geq 0$, and thus (1.10.1) is a strongly degenerate parabolic problem. The scalar conservation law $u_t + f(u)_x = 0$ is a special example of this type of problems.

Independently of the smoothness of the initial data, due to the degeneracy of the diffusion, jumps may form in the solution u. Therefore we consider solutions in the weak sense, i.e.,

Definition 1.10.1. *Set $\Pi_T = (0,T)\times\mathbb{R}$, a function $u(t,x) \in L^\infty((0,T);L^1(\mathbb{R}))\cap L^\infty(\Pi_T)$ is a weak solution of the initial value problem* (1.10.1) *if it satisfies*

***D**.1 $A(u)$ is continuous and $A(u)_x \in L^\infty(\Pi_T)$.*

***D**.2 For all test functions $\varphi \in \mathcal{D}(\Pi_T)$*

$$\iint_{\Pi_T} u\varphi_t + f(u)\varphi_x + A(u)\varphi_{xx}\,dxdt = 0. \tag{1.10.2}$$

***D**.3 The initial condition is satisfied in the L^1-sense*

$$\lim_{t\downarrow 0} \int_{\mathbb{R}} |u(t,x) - u_0(x)|\,dx = 0.$$

In view of the existence theory, the condition **D**.1 is natural, and thanks to this we can replace (1.10.3) by

$$\iint_{\Pi_T} u\varphi_t + (f(u) - A(u)_x)\,\varphi_x\,dxdt = 0. \tag{1.10.3}$$

If A is constant on a whole interval, then weak solutions are not uniquely determined by their initial data, and one must impose an additional entropy condition to single out the physically relevant solution. A weak solution satisfies the entropy condition if

$$\varrho(u)_t + q(u)_x + r(u)_{xx} \leq 0 \text{ in } \mathcal{D}'(\Pi_T), \tag{1.10.4}$$

for all convex, twice differentiable functions $\varrho : \mathbb{R} \to \mathbb{R}$, where q and r are defined by

$$q'(u) = \varrho'(u)f'(u), \text{ and } r'(u) = \varrho'(u)A'(u).$$

Via a standard limiting argument this implies that (1.10.4) holds for the Kružkov entropies $\varrho(u) = |u - c|$ for all constants c. We say that a weak solution satisfying the entropy condition is an entropy solution.

The aim of this work is to derive a **convergence rate estimate** for the approximate solutions to degenerate problems. For conservation laws (very degenerate problems), the convergence rate for monotone methods has long been known to be $\Delta x^{1/2}$ [36], and this is also optimal for discontinuous solutions. For non-degenerate problems, the solution operator (taking initial data to the corresponding solution) has a strong smoothing effect, and truncation analysis applies. Hence difference methods produces approximations converging at the formal order of the scheme.

1.10.1 Summary of the general results

In this section we state the main results of Paper IV. To begin with, we collect some useful information about entropy solutions in the following, for a proof see [34]. Let the signum function be defined as

$$\operatorname{sign}(\sigma) = \begin{cases} -1 & \sigma < 0, \\ 0 & \sigma = 0, \\ 1 & \sigma > 0, \end{cases}$$

and its regularized counterpart, $\operatorname{sign}_\varepsilon$, defined as

$$\operatorname{sign}_\varepsilon(\sigma) = \begin{cases} \operatorname{sign}(\sigma) & |\sigma| > \varepsilon, \\ \sin\left(\frac{\pi\sigma}{2\varepsilon}\right) & \text{otherwise}, \end{cases}$$

where $\varepsilon > 0$.

Theorem 1.10.1. *If $u_0 \in B.V(\mathbb{R}) \cap L^1(\mathbb{R})$, then there exists a unique entropy solution u satisfying*

$$\iint_{\Pi_T} |u-c|\,\varphi_t + \operatorname{sign}(u-c)(f(u)-f(c))\varphi_x + |A(u)-A(c)|\,\varphi_{xx}\,dxdt \geq 0, \tag{1.10.5}$$

for all constants c and all non-negative test functions in $\mathcal{D}'(\Pi_T)$. Furthermore, the following limits hold,

$$\begin{aligned} \iint_{\Pi_T} |u-c|\,\varphi_t + &\operatorname{sign}(u-c)\,(f(u)-f(c)-A(u)_x)\,\varphi_x \\ &= \lim_{\varepsilon\downarrow 0} \iint_{\Pi_T} |A(u)_x|^2 \operatorname{sign}'_\varepsilon\,(A(u)-A(c))\;\varphi\,dtdx, \end{aligned} \tag{1.10.6}$$

$$\lim_{\varepsilon\downarrow 0} \iint_{\Pi_T} (f(u)-f(c))\,A(u)_x \operatorname{sign}'_\varepsilon\,(A(u)-A(c))\,\varphi\,dtdx = 0, \tag{1.10.7}$$

for all non-negative test functions φ.

We consider a semi-discrete approximation, where space is discrete, but time continuous. Let Δx be some small parameter, and set $x_j = j\Delta x$ and $x_{j+1/2} = (j+1/2)\Delta x$ for $j \in \mathbb{Z}$. Set $I_j = (x_{j-1/2}, x_{j+1/2}]$. The discrete derivatives $D^\pm$ are defined by

$$D^\pm \sigma_j = \pm \frac{\sigma_{j\pm 1} - \sigma_j}{\Delta x}.$$

Our scheme is defined by

$$\begin{cases} \frac{d}{dt}u_j(t) + D^- F_{j+1/2} = D^- D^+ A_j, & t > 0, \\ u_j(0) = \frac{1}{\Delta x}\int_{I_j} u_0(x)\,dx, \end{cases} \tag{1.10.8}$$

for $j \in \mathbb{Z}$. Here $F_{i+1/2}$ is some consistent numerical flux

$$F_{j+1/2} = F\left(u_j, u_{j+1}\right) \text{ and } A_j = A\left(u_j\right).$$

In order to define an approximation on the whole of Π_T, we let $u_{\Delta x}$ be the piecewise linear interpolant given by

$$u_{\Delta x}(x,t) = u_j(t) + D^+ u_j(t)\left(x - x_j\right), \quad \text{for } x \in [x_j, x_{j+1}],$$

and with a slight abuse of notation we define u_j to be the piecewise constant function

$$u_j(x) = u_j \quad \text{for } x \in (x_{j-1/2}, x_{j+1/2}].$$

We have some useful estimates for $u_j(t)$:

- a uniform L^∞ bound.
- a uniform total variation bound.

and the following two estimates for the discrete total flux term $F_{j+1/2}(t) - D^+ A\left(u_j(t)\right)$:

- a uniform L^∞ bound.
- a uniform total variation bound.

See [35] for more details about the proof of above estimates. Our main result in this paper is the following:

Main Theorem. Let u be the unique entropy solution to (1.10.1) and $u_{\Delta x}$ be as defined by (1.10.8). Choose a constant

$$M > \max_{|u| < \|u_0\|_{L^\infty(\mathbb{R})}} \left|f'(u)\right|,$$

and another constant $L > MT$, where $T > 0$. Then there exists a constant C, independent of Δx, but depending on f, L, T and u_0, such that

$$\int_{-L+Mt}^{L-Mt} \left|u(t,x) - u_{\Delta x}(t,x)\right| dx \leq C\Delta x^{1/11} \quad \text{for } t \leq T.$$

As a by-product of our method of proof we get an improved rate if the diffusion is **linear**. The significance of this rate is that is independent of the size of the diffusion, which in this case is η .

Main Corollary. Let u be the unique solution to the viscous regularization

$$u_t + f(u)_x = \eta u_{xx}. \quad t > 0, \quad u(x,0) = u_0(x),$$

and let $u_{\Delta x}$ be defined by (1.10.8) with $A(u) = \eta u$. Then there exists a constant C, independent of Δx and η, but depending on f, L, T and u_0, such that

$$\int_{-L+Mt}^{L-Mt} |u(t,x) - u_{\Delta x}(t,x)| \, dx \leq C\Delta x^{1/2} \quad \text{for } t \leq T.$$

Proof. (Sketch only)

First note that, instead of discretizing (1.10.1), we shall discretize the following regularized equation

$$u_t^\eta + f\left(u^\eta\right)_x = \left(A\left(u^\eta\right) + \eta u^\eta\right)_{xx}, \; t > 0, \quad u^\eta(0,x) = u_0(x), \tag{1.10.9}$$

and let η tend to zero in a suitable manner. Since in [34], it was established that for $t < T$

$$\left\|u(t,\cdot) - u^\eta(t,\cdot)\right\|_{L^1(\mathbb{R})} \leq C\sqrt{\eta}, \tag{1.10.10}$$

it suffices to compare u^η and our approximate solution.

The main idea behind the proof is mainly "doubling of the variables" argument. Rather than starting with the entropy condition (1.10.5), we will start with the argument leading up to this condition. To do that, set

$$\psi_\varepsilon(u,c) = \int_c^u \operatorname{sign}_\varepsilon\left(A(z) - A(c)\right) dz.$$

This is a convex entropy for all constants c. Although $\psi_\varepsilon(u,c) \approx |u-c|$ but since ψ_ε is not symmetric in u and c, this makes difficult to work with when doubling the variables. But nevertheless, one can prove the following equality:

$$\begin{aligned}
&\int_{\Pi_T^2} |u - u_{\Delta x}| \, \varphi_s + \operatorname{sign}_\varepsilon\left(A(u) - A\left(u_{\Delta x}\right)\right)\left(f(u) - f\left(u_{\Delta x}\right)\right)\varphi_y \, dX \\
&\quad = \int_{\Pi_T^2} \Big[\operatorname{sign}_\varepsilon'\left(A(u) - A\left(u_{\Delta x}\right)\right)\left(\left(A(u)_y\right)^2 - A(u)_y A\left(u_{\Delta x}\right)_x\right)\varphi \\
&\qquad\qquad - \left|A(u) - A\left(u_{\Delta x}\right)\right|_\varepsilon \left(\varphi_{yy} + \varphi_{xy}\right) \\
&\qquad\qquad + \operatorname{sign}_\varepsilon'\left(A(u) - A\left(u_{\Delta x}\right)\right)\left(f(u) - f\left(u_{\Delta x}\right)\right) A(u)_y \varphi \\
&\qquad\qquad + \left(\psi_\varepsilon\left(u, u_{\Delta x}\right) - |u - u_{\Delta x}|\right)\varphi_s \Big] \, dX,
\end{aligned} \tag{1.10.11}$$

where $dX = dydsdxdt$ and $|a|_\varepsilon = \int_0^a \operatorname{sign}_\varepsilon(z) dz$.

Now next aim is to obtain an analogous estimate for the difference approximation $u_{\Delta x}$.

One can prove the following equality holds:

$$\begin{aligned}
&\int_{\Pi_T^2} |u_{\Delta x} - u|\,\varphi_t + \operatorname{sign}_\varepsilon\left(A\left(u_{\Delta x}\right) - A(u)\right)\left(f\left(u_{\Delta x}\right) - f\left(u\right)\right)\varphi_x\, dX \\
&= \int_{\Pi_T^2} \operatorname{sign}'_\varepsilon\left(A\left(u_{\Delta x}\right) - A(u)\right)\left(\left(A\left(u_{\Delta x}\right)_x\right)^2 - A\left(u_{\Delta x}\right)_x A(u)_y\right)\varphi\, dX \\
&\qquad - \int_{\Pi_T^2} \left|A\left(u_{\Delta x}\right) - A(u)\right|_\varepsilon \left(\varphi_{xx} + \varphi_{xy}\right)\, dX \\
&\qquad + \int_{\Pi_T^2} \text{“Error terms”}\, dX.
\end{aligned} \tag{1.10.12}$$

Now adding (1.10.11) and (1.10.12), and after some manipulations one can show that the following inequality holds.

$$\begin{aligned}
&\int_{\Pi_T^2} \Big[|u_{\Delta x} - u|\left(\varphi_t + \varphi_s\right)) \\
&\qquad + \operatorname{sign}_\varepsilon\left(A\left(u_{\Delta x}\right) - A(u)\right)\left(f\left(u_{\Delta x}\right) - f(u)\right)\left(\varphi_x + \varphi_y\right) \\
&\qquad + \left|A(u_{\Delta x}) - A(u)\right|_\varepsilon \left(\varphi_{xx} + 2\varphi_{xy} + \varphi_{yy}\right)\Big]\, dX \\
&\geq \int_{\Pi_T^2} \operatorname{sign}'_\varepsilon\left(A(u) - A\left(u_{\Delta x}\right)\right)\left(f(u) - f\left(u_{\Delta x}\right)\right) A(u)_y \varphi\, dX \\
&\quad + \int_{\Pi_T^2} \left(\psi_\varepsilon\left(u, u_{\Delta x}\right) - |u - u_{\Delta x}|\right)\varphi_s\, dX \\
&+ \int_{\Pi_T^2} \text{“Error terms”}\, dX. \\
&=: \int_{\Pi_T^2} \mathcal{Q}_1 + \mathcal{Q}_2\, dX + \int_{\Pi_T^2} \text{“Error terms”}\, dX
\end{aligned} \tag{1.10.13}$$

We shall specify now a “suitable” nonnegative test function $\varphi = \varphi(t, x, s, y)$ defined in $\Pi_T \times \Pi_T$. In order to manipulate the first term on the left of (1.10.13), we have used the following two facts:

$$\begin{aligned}
&\iint |u(x,t) - u(y,t)|\,\omega_r(x-y)\, dxdy \leq Cr \\
&\text{and } \iint |u(x,s) - u(x,t)|\,\omega_{r_0}(t-s)\, dxds \leq Cr_0,
\end{aligned} \tag{1.10.14}$$

for some standard mollifier ω and $\omega_r(x) = \frac{1}{r}\omega(\frac{x}{r})$. One can also show that the second and third terms on the left of (1.10.13) can be bounded by $C(r_0 + r + \alpha + \alpha_0)$, where all these parameters are coming from the particular choice of the test function ϕ.

In order to estimate the integral of $\mathcal{Q}_2$, we have used the facts that $A' \geq \eta$ and $|\psi_\varepsilon(a,b) - |a-b|| \leq C\frac{\varepsilon}{\eta}$. On the other hand, we have used the coarea formula in order to estimate the integral of $\mathcal{Q}_1$. Observe that

$$\left\{\operatorname{sign}_\varepsilon\left(A(u_{\Delta x}) - A(u)\right) = \sigma\right\} \;\Rightarrow\; \left\{|f(u_{\Delta x}) - f(u)| \leq \frac{M\varepsilon\sigma}{\eta}\right\}$$

for $\sigma \in [-1, 1]$.

Now the final task is to estimate all the "error terms" in an appropriate manner. Finally, combining all these estimates one can show that the estimate stated in the Main theorem holds.

□

1.10.2 Summary of numerical result

In order to test the unlikely optimality of the convergence rate of our main theorem, we compute the numerical convergence rate of an example. Consider the following initial value problem

$$\begin{cases} u_t = A(u)_{xx} & \text{for } t > 0 \text{ and } x \in (-\pi/2, \pi), \quad A(u) = \frac{1}{2}\left(\max\{u, 0\}\right)^2 \\ u(x, 0) = \sin(x), & x \in [-\pi/2, \pi], \end{cases} \tag{1.10.15}$$

supplemented with the boundary conditions

$$\partial_x A(u(t, x)) = 0 \quad \text{for } t > 0 \text{ and } x = -\pi/2,\ x = \pi.$$

We have used the Euler method to integrate the system of ordinary differential equations (1.10.8), resulting in the update formula

$$u_j((n+1)\Delta t) = u_j(n\Delta t) + \Delta t D^- D^+ A_j(n\Delta t).$$

In Figure 1.10.1 we show the solution in the (x, t) plane and a snapshot of u at $t = 1$, for an approximation using 400 grid points in the interval $(-\pi/2, \pi)$.

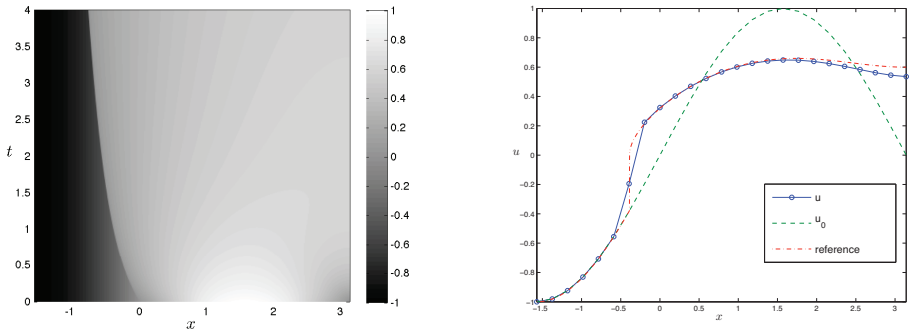

Figure 1.10.1: An approximate solution to (5.4.1) using 400 grid points. Left: u in the (x, t) plane for $t \in [0, 4]$. Right: an approximation to $u(1, x)$ using 25 grid points, a reference solution computed using 4000 grid points and the initial data.

1.11 Concluding remarks

We have considered the magnetic induction equations that arise as a submodel in the MHD equations of plasma physics. We considered SBP-SAT based finite difference schemes for the initial-boundary value problem corresponding to the magnetic induction equations and magnetic induction equations with resistivity. We used SBP finite difference operators to approximate spatial derivatives and a SAT technique for implementing boundary conditions. The resulting schemes were energy stable and high order accurate.

In future we plan to extend this SBP-SAT framework to more realistic models involving induction equations (e.g. MHD). The mathematical model for the atmospheric dynamics in the context of MHD theory is highly nonlinear; it is almost impossible to seek meaningful analytical solutions for realistic physical problems. Therefore, we need to utilize appropriate numerical methods to seek approximate solutions which are known as numerical simulations. It is well-known that the treatment of appropriate boundary conditions is the key to the success of MHD simulation of a realistic physical situation. To proceed otherwise will lead to an erroneous physical solution and misinterpretation of the observed physical features. Main aim is to investigate and design stable high order numerical boundary closures for the MHD equations. In a more general context, we have been trying to construct an entropy conservative/stable scheme in the presence of boundaries for general nonlinear conservation laws.

In the recent years, spectral method have becomes one of the standard tools for the approximate solution of nonlinear partial differential equations. It is well known that spectral methods enjoy high order of accuracy as long as underlying solution is smooth. We have been working on the convergence of a fully discrete spectral scheme for the Kawahara equation (1.9.1). We are analyzing a fully discrete spectral method for the numerical solution of the initial- and periodic boundary-value problem for Kawahara equation. The equation is discretized in space by the standard Fourier-Galerkin spectral method and in time by the explicit leap-frog scheme. For the resulting fully discrete, conditionally stable scheme we expect to prove an L^2-error bound of spectral accuracy in space and of second-order accuracy in time.

In paper IV, we have shown that the L^1_{loc} difference between the approximate solution and the unique entropy solution of nonlinear degenerate convection-diffusion equation converges at a rate $\mathcal{O}(\Delta x^{1/11})$, where Δx is the spatial mesh size. This rate of convergency is certainly not optimal. We plan to continue investigating the rate of convergence for degenerate convection-diffusion equations in a different framework, based on the kinetic formulation. This approach does not make use of Kruzkov entropies and doubling of variables. It uses in a fundamental way the entropy defect measure appearing in the kinetic formulation. This measure plays a central role for proving error estimates.

Bibliography

[1] Helge Holden and Nils Henrik Risebro. Front tracking for hyperbolic conservation laws. *Volume 152 of Applied Mathematical Sciences.*, Springer-Verlag, New York, 2005.

[2] N. Besse and D. Kröner. Convergence of the locally divergence free discontinuous Galerkin methods for induction equations for the 2D-MHD system. *M2AN Math. Model. Num. Anal* 39(6):1177-1202, 2005.

[3] K.G. Powell. An approximate Riemann solver for magneto-hydro dynamics (that works in more than one space dimension). Technical report, 94 -24, ICASE, Langley, VA, 1994.

[4] R. Bürger, F. Concha. Mathematical model and numerical simulation of the settling of flocculated suspensions,. Preprint, University of Stuttgart (1997).

[5] R. Bürger, W. L. Wendland Mathematical problems in sedimentation. *Proceedings of the third summer conference " numerical modelling in continuum mechanics"*, Prague (Czech Republic), 1997.

[6] G. Chavent and J. Jaffre. Mathematical models and finite elements for reservoir simulation. North Holland, Amsterdam, 1986.

[7] O. A. Oleinik, S. N. Kruzkov. Quasilinear second order equations with many independent variables. Russian Math. Surveys 16 (1961), 105-146.

[8] B .H. Gilding. Improved theory for a nonlinear degenerate parabolic equation. *Ann. Scuola Norm. Sup. Pisa Cl. Sci.*, 16(4): 165-224, 1989.

[9] A. S. Kalashnikov. Some results of the qualitative theory of non-linear degenerate second-order parabolic equations. *Russian Math. Surv.*, 42 : 169-222, 1987.

[10] H. Brezis and M. G. Crandall. Uniqueness of solutions of the initial value problem for $u_t - \Delta\phi(u) = 0$. *J. Math. Pures et Appl.*, 58 (1979), 153-163.

[11] J. Carrillo. Entropy solutions for nonlinear degenerate problems. *Arch. Ration. Mech. Anal.*, 147(4): 269-361, 1999.

[12] K. H. Karlsen and N. H. Risebro On the uniqueness and stability of entropy solutions of nonlinear degenerate parabolic equations with rough coefficients. *Discrete Contin. Dyn. Syst.*, 9(5): 1081-1104, 2003.

[13] S. N. Kruzkov. First order quasilinear equations with several independent variables. *Mat. Sb. (N.S).*, 81(123): 228-255, 1970.

[14] A. I. Volpert. Generalized solutions of degenerate second-order quasilinear parabolic and elliptic equations. *Adv. Differential equations.*, 5(10-12): 1493-1518, 2000.

[15] A. I. Volpert and S. I. Hudjaev. The Cauchy problem for second order quasilinear degenerate parabolic equations. *Mat. Sb. (N.S).*, 78(120): 374-396, 1969.

[16] Hunter, J.K, Scheurle, J.: Existence of perturbed solitary wave solutions to a model equation for water waves. *Physica D.*, 32, 253-268, 1988.

[17] Kawahara, T.: Oscillatory solitary waves in dispersive media. *J. Phys. Soc. Japan.*, 33: 260-264, 1972.

[18] Kichenassamy, S., Olver, P. J.: Existence and nonexistence of solitary wave solutions to higher-order model evolution equations. *SIAM J. Math. Anal.*, 23: 1141-1166, 1992.

[19] T. Kato.: On the Korteweg-de Vries equation. *Manuscripta Math.*, 28: 89-99, 1979.

[20] J. Ponce.: Regularity of solutions to nonlinear dispersive equations. *J. Diff. Eq.*, 78: 122-135, 1989.

[21] Gleb G. Doronin, Nikolai A. Larkin.: Well and ill-posed problems for the KdV and Kawahara equations. *Bol. Soc. Paran. Mat.*, v. 26 1-2: 133-137, 2008.

[22] Hua WANG., Shang Bin CUI., Dong Gao DENG.: Global existence of solutions for the Kawahara equation in Sobolev spaces of negative indices. *Acta Mathematica Sinica.*, vol. 23 No. 8 : 1435-1446, 2007.

[23] Shang Bin CUI., Dong Gao DENG., Shuang Ping TAO.: Global existence of solutions for the Cauchy problem of the Kawahara equation with L^2 initial data. *Acta Mathematica Sinica.*, vol. 22 No. 5 : 1457-1466, 2006.

[24] Jennifer Gorsky, A. Alexandrou Himonas,: Well-posedness of KdV with higher dispersion. *Mathematics and Computors in Simulation.*, 80 : 173-183, 2009.

[25] R. J. LeVeque: Finite volume methods for hyperbolic problems. *Cambridge university press.*, Cambridge 2002.

[26] Saul Abarbanel and Alina E. Chertock. Strict stability of high-order compact implicit finite-difference schemes: The role of boundary conditions for hyperbolic pdes, I. *J. Comput. Phys.*, 160, 2000.

[27] Saul Abarbanel, Alina E. Chertock and Amir Yefet. Strict stability of high-order compact implicit finite-difference schemes: The role of boundary conditions for hyperbolic pdes, II. *I. J. Comput. Phys.*, 160, 2000.

[28] M. H. Carpenter, D. Gottlieb, and S. Abarbanel. Time-stable boundary conditions for finite-difference schemes solving hyperbolic systems: Methodology and application to high-order compact schemes. *J. Compt. Phys.*, 111(2), 1994.

[29] H.-O. Kreiss and G. Scherer. Finite element and finite difference methods for hyperbolic partial differential equations. *Mathematical Aspects of Finite El- ements in Partial Differential Equations.*, Academic Press, Inc., 1974.

[30] H.-O. Kreiss and G. Scherer. On the existence of energy estimates for difference approximations for hyperbolic systems. *Technical report, Dept. of Scientific Computing* , Uppsala University, 1977.

[31] Bo Strand. Summation by Parts for Finite Difference Approximations for $\frac{d}{dx}$ *J. Compt. Phys.*, 110, 1994.

[32] Bo Strand. High-order difference approximations for hyperbolic initial boundary value problems. *PhD thesis, Uppsala University, Dep. of Scientific Computing .*, Uppsala Univ., Uppsala, Sweden, 1996.

[33] M. Torrilhon and M. Fey. Constraint-preserving upwind methods for multidimensional advection equations. *SIAM. J. Num. Anal.*, 42(4): 1694-1728, 2004.

[34] S. Evje and K. H. Karlsen. An error estimate for viscous approximate solutions of degenerate parabolic equations. *J. Nonlinear Math. Phys.*, 9(3): 262-281, 2002.

[35] S. Evje and K. H. Karlsen. Monotone difference approximations of BV solutions to degenerate convection-diffusion equations. *SIAM J. Numer. Anal.*, 37(6): 1838-1860 (electronic), 2000.

[36] N. N. Kuznetsov. The accuracy of certain approximate methods for the computation of weak solutions of a first order quasilinear equation. *Ž. Vyčisl. Mat. i Mat. Fiz.*, 16(6): 1489-1502, 1627, 1976.

[37] K.G. Powell, P.L. Roe. T.J. Linde, T.I. Gombosi and D.L. De Zeeuw, A solution adaptive upwind scheme for ideal MHD. J. Comp. Phys, 154(2), 284 - 309, 1999

[38] S.K. Godunov. The symmetric form of magnetohydrodynamics equation. *Num. Meth. Mech. Cont. Media*, 1:26-34, 1972.

[39] M. Torrilhon and M. Fey. Constraint-preserving upwind methods for multidimensional advection equations. *SIAM. J. Num. Anal.*, 42(4):1694-1728, 2004.

[40] G. Toth. The div$B = 0$ constraint in shock capturing magnetohydrodynamics codes. *J. Comp. Phys.*,161:605-652, 2000.

[41] J.U. Brackbill and D.C. Barnes. The effect of nonzero div$B$ on the numerical solution of the magnetohydrodynamic equations. *J. Comp. Phys.*, 35:426-430, 1980.

[42] K.G. Powell. An approximate Riemann solver for magneto-hydro dynamics (that works in more than one space dimension). Technical report, 94 -24, ICASE, Langley, VA, 1994.

[43] D.S. Balsara and D. Spicer. A staggered mesh algorithm using high order Godunov fluxes to ensure solenoidal magnetic fields in magnetohydrodynamic simulations. *J. Comp. Phys.*, 149(2):270-292, 1999.

[44] N. Besse and D. Kröner. Convergence of the locally divergence free discontinuous Galerkin methods for induction equations for the 2D-MHD system. *M2AN Math. Model. Num. Anal* 39(6):1177-1202, 2005.

[45] W. Dai and P.R. Woodward. A simple finite difference scheme for multi-dimensional magnetohydrodynamic equations. *J. Comp. Phys.*, 142(2):331-369, 1998.

[46] C. Evans and J.F. Hawley. Simulation of magnetohydrodynamic flow: a constrained transport method. *Astrophys. J.*, 332:659, 1998.

[47] F. Fuchs, K.H. Karlsen, S. Mishra and N.H. Risebro. Stable upwind schemes for the Magnetic Induction equation. *Preprint,* Submitted.

[48] D.S. Ryu, F. Miniati, T.W. Jones and A. Frank. A divergence free upwind code for multidimensional magnetohydrodynamic flows. *Astrophys. J.*, 509(1):244-255, 1998.

[49] A. Sjöberg.: On the Korteweg-de Vries equation: Existence and uniqueness. *J. Math. Anal. Appl.*, 29: 569-579, 1970.

[50] Juan Carlos Ceballos., Mauricio Sepulveda., Octavio Paulo Vera Villagran.: The Korteweg-de Vries-Kawahara equation in a bounded domain and some numerical results. *Applied Matheamatics and Computation.*, 190: 912-936, 2007.

2

Higher order finite difference schemes for the Magnetic Induction equations

U. Koley, S. Mishra, N. H. Risebro, M. Svärd
BIT Numer Math (2009) 49:375-395

Keywords: conservation laws, induction equations, summation-by-parts operator, boundary conditions, finite difference schemes, high order of accuracy

Abstract

We describe high order accurate and stable finite difference schemes for the initial-boundary value problem associated with the magnetic induction equations. These equations model the evolution of a magnetic field due to a given velocity field. The finite difference schemes are based on Summation by Parts (SBP) operators for spatial derivatives and a Simultaneous Approximation Term (SAT) technique for imposing boundary conditions. We present various numerical experiments that demonstrate both the stability as well as high order of accuracy of the schemes.

2.1 Introduction

The magnetic induction equations are a special form of the Maxwell's equations that describe the evolution of the magnetic field under the influence of a given velocity field. These equations arise in a wide variety of applications in plasma physics, astrophysics and electrical engineering. One important application are the equations of magneto-hydro dynamics (MHD). These equations combine the Euler equations of gas dynamics with the magnetic induction equations. Our goal in this paper is to describe stable and high-order accurate numerical schemes for the magnetic induction equations.

We start with a brief description of how the equations are derived. Let the magnetic field and given velocity field be denoted by $\mathbf{B}$ and $\mathbf{u}$ respectively. Faraday's law for the magnetic flux across a surface $\mathbf{S}$ bounded by a curve $\partial\mathbf{S}$ is given by (see [18]),

$$\frac{d}{dt}\int_S \mathbf{B}\cdot\mathbf{dS} = \oint_{\partial S} \mathbf{E}\cdot dl.$$

Using the Stokes theorem and the fact that the electric field, $\mathbf{E}$, in a co-moving frame is zero and the magnetic resistivity is zero, Faraday's law takes the form,

$$\frac{\partial \mathbf{B}}{\partial t} + \mathrm{div}(\mathbf{u} \otimes \mathbf{B} - \mathbf{B} \otimes \mathbf{u}) = -\mathbf{u}\mathrm{div}(\mathbf{B}). \tag{2.1.1}$$

Using simple vector identities, (2.1.1) can be rewritten as,

$$\partial_t \mathbf{B} + \mathrm{curl}(\mathbf{B} \times \mathbf{u}) = -\mathbf{u}\mathrm{div}(\mathbf{B}). \tag{2.1.2}$$

Magnetic monopoles have never been observed in nature. As a consequence, the magnetic field is always assumed to be divergence free, i.e., $\mathrm{div}(\mathbf{B}) = 0$. Hence, it is common to set the right-hand side of (2.1.2) to zero and couple the induction equation with the divergence constraint in order to obtain

$$\begin{aligned} \partial_t \mathbf{B} + \mathrm{curl}(\mathbf{B} \times \mathbf{u}) &= 0, \\ \mathrm{div}(\mathbf{B}) &= 0,\ \mathbf{B}(x,0) = \mathbf{B}_0(x). \end{aligned} \tag{2.1.3}$$

This form (2.1.3) is commonly used in the literature as the appropriate form of the magnetic induction equations to study and discretize. It is easy to see that (2.1.3) is hyperbolic but not strictly hyperbolic. An important tool in the analysis of hyperbolic system of equations is the derivation of energy estimates. The usual procedure in deriving energy estimates consists of symmetrizing the hyperbolic system. It is not possible to symmetrize (2.1.3) without explicitly using the divergence constraint. Hence, it is difficult to obtain energy stability starting from (2.1.3).

On the other hand, we can use the following vector identity

$$\begin{aligned} \mathrm{curl}(\mathbf{B} \times \mathbf{u}) &= \mathbf{B}\mathrm{div}\mathbf{u} - \mathbf{u}\mathrm{div}(\mathbf{B}) + (\mathbf{u} \cdot \nabla)\,\mathbf{B} - (\mathbf{B} \cdot \nabla)\,\mathbf{u} \\ &= \left(u^1\mathbf{B}\right)_x + \left(u^2\mathbf{B}\right)_y + \left(u^3\mathbf{B}\right)_z - \mathbf{u}\mathrm{div}(\mathbf{B}) - (\mathbf{B} \cdot \nabla)\mathbf{u}, \end{aligned}$$

and rewrite (2.1.1) in the non-conservative symmetric form,

$$\begin{aligned} \partial_t \mathbf{B} + (\mathbf{u} \cdot \nabla)\,\mathbf{B} &= -\mathbf{B}(\mathrm{div}\mathbf{u}) + (\mathbf{B} \cdot \nabla)\mathbf{u} \\ &= M(D\mathbf{u})\mathbf{B}, \end{aligned} \tag{2.1.4}$$

where the $D\mathbf{u}$ denotes the gradient of $\mathbf{u}$ and the matrix $M(D\mathbf{u})$ is given by

$$M(D\mathbf{u}) = \begin{pmatrix} -\partial_y u^2 - \partial_z u^3 & \partial_y u^1 & \partial_z u^1 \\ \partial_x u^2 & -\partial_x u^1 - \partial_z u^3 & +\partial_z u^2 \\ \partial_x u^3 & \partial_y u^3 & -\partial_x u^1 - \partial_y u^2 \end{pmatrix}.$$

Introducing the matrix,

$$C = -\begin{pmatrix} \partial_x u^1 & \partial_y u^1 & \partial_z u^1 \\ \partial_x u^2 & \partial_y u^2 & \partial_z u^2 \\ \partial_x u^3 & \partial_y u^3 & \partial_z u^1 \end{pmatrix},$$

(2.1.1) can also be written in the following "conservative" symmetric form,

$$\partial_t \mathbf{B} + \partial_x \left(A^1\mathbf{B}\right) + \partial_y \left(A^2\mathbf{B}\right) + \partial_z \left(A^3\mathbf{B}\right) + C\mathbf{B} = 0, \tag{2.1.5}$$

where $A^i = u^i I$ for $i = 1, 2, 3$. Note that the symmetrized matrices in (2.1.5) are diagonal and that the only coupling in the equations is through the lower order terms. These symmetrized forms are in the same spirit as the non-linear symmetrized forms of MHD equations introduced in [8].

Furthermore, by taking divergence on both sides of (2.1.2) we get

$$(\mathrm{div}(\mathbf{B}))_t + \mathrm{div}\,(\mathbf{u}\mathrm{div}(\mathbf{B})) = 0. \tag{2.1.6}$$

Hence, if $\mathrm{div}(\mathbf{B}_0(\mathbf{x})) = 0$, also $\mathrm{div}(\mathbf{B}(\mathbf{x}, t)) = 0$ for $t > 0$. This implies that all the above forms (2.1.5), and (2.1.3) are equivalent (at least for smooth solutions). Introducing the space H^{div} as

$$H^{\mathrm{div}}(\mathbb{R}^3) = \left\{ \mathbf{w} : \mathbb{R}^3 \to \mathbb{R}^3 \;\middle|\; |\mathbf{w}| \in L^2(\mathbb{R}^3),\ \ \mathrm{div}(\mathbf{w}) \in L^2(\mathbb{R}^3) \right\},$$

we have the following theorem:

Theorem 2.1.1. *Assume that the velocity field* $\mathbf{u}$ *is sufficiently smooth, and that* $\mathbf{B}_0 \in H^{\mathrm{div}}(\mathbb{R}^3)$*. Then there exists a unique weak solution* $\mathbf{B} \in C([0, T]; H^{\mathrm{div}}(\mathbb{R}^3))$ *of (2.1.5). The solution* $\mathbf{B}$ *satisfies the energy estimate,*

$$\|\mathbf{B}(\cdot, T)\|_{H^{\mathrm{div}}(\mathbb{R}^3)} \leq C_T \|\mathbf{B}_0\|_{H^{\mathrm{div}}(\mathbb{R}^3)}$$

The constant C_T *depends only on the final time* T*. Furthermore, if* $\mathrm{div}(\mathbf{B}_0) = 0$*, then the physical form (2.1.1) and the symmetric form (2.1.5) are equivalent to the constrained form (2.1.3), i.e.,* $\mathbf{B}$ *is also the unique weak solution of (2.1.3).*

The proof of the above theorem uses the energy estimate and we will provide a sketch of the proof for the two-dimensional version of the equations together with boundary conditions later in this paper.

Even though the magnetic induction equations are linear, the presence of variable coefficients and lower order terms means that general closed form solutions are not available. Hence, one has to design suitable numerical schemes for these equations. Furthermore, since these equations appear as a sub-model in the MHD equations, the design of stable and high-order accurate numerical schemes for the induction equations can lead to the design of robust schemes for the non-linear MHD equations.

Most of the attention in the literature has been focused on the constrained form (2.1.3). The key issue in the design of a suitable numerical scheme to approximate (2.1.3) has been the treatment of the divergence constraint. A widely used approach has been to employ projection methods based on a Hodge decomposition of the magnetic field. A base (finite difference or finite volume) scheme is used to evolve the magnetic field. The evolved field, which need not be divergence free, is then corrected for divergence errors by solving an elliptic equation (see [4]). The resulting method is computationally expensive, as the elliptic equation has to be solved at every time step.

Another common approach is to discretize (2.1.3) such that some particular form of discrete divergence is preserved at each time step (see [11]). This approach is equivalent to staggering the velocity and magnetic fields in each direction (see [4, 1, 20, 5] and a detailed comparison in [12]). Some of these schemes are proved to be von Neumann stable

in the special case of constant velocity fields. No stability analysis is available either in the case of variable velocity fields or for problems with boundary conditions. These schemes also involve wider stencils than what is required for a standard finite difference scheme.

Despite all the attempts at finding a suitable discretization of (2.1.3) and preserving a special form of discrete divergence, it is not clear as to whether such an approach is appropriate. Furthermore, there are many different choices for the discrete divergence operator and preserving some form of discrete divergence exactly does not lead to preservation or even keeping divergence errors small for a different form. The main aim should be to design a stable scheme to approximate magnetic fields and it is not clear whether preserving divergence in a particular discrete form helps. One reason for the difficulties in proving stability of discretizations for (2.1.3) with general velocity fields may lie in the very form of these equations. As remarked earlier, (2.1.3) are not symmetrizable directly and thus one cannot obtain energy estimates in this form. This remains true for discretizations of (2.1.3).

A different approach consisting of discretizing the physical form (2.1.1) was proposed in [17] for the non-linear MHD equations. Adapting this to (2.1.1) implies using a standard upwind scheme for the convection part and a centered discretization of the source terms. From (2.1.6), one can expect that divergence errors will be transported out of the domain for transparent boundary conditions. This approach does not imply stability either and can lead to oscillations as reported in [5]. A discontinuous Galerkin based discretization of the symmetric form (2.1.5) was proposed in [2].

In a recent paper [5], the authors discretized the symmetric form (2.1.4) by using a first order accurate upwind finite difference scheme. The resulting scheme also implied an upwind discretization of the convection term in (2.1.1) with an upwind discretization of the source term. This scheme was shown to be energy stable even with variable velocity fields and to be TVD for constant velocity fields.

Furthermore, boundary conditions were not considered either in [5] or any of the aforementioned papers. High-order accurate schemes will lead to much better resolution of interesting solution features and a stable discretization of the boundary conditions (while still preserving high order of accuracy) is desirable.

Our aim in this paper is to design stable and high-order accurate schemes for initial-boundary value problems corresponding to the magnetic induction equations by discretizing the non-conservative symmetric form (2.1.4). The spatial derivatives are approximated by second and fourth-order SBP (Summation-By-Parts) operators. The boundary conditions are weakly imposed by using a SAT (Simultaneous Approximation Term) and time integration is performed by standard Runge-Kutta schemes. The SBP-SAT framework has been used to obtain stable and accurate high order schemes for a wide variety of hyperbolic problems in recent years. See [22] and the references therein for more details.

The SBP-SAT schemes use centered finite difference stencils in the interior, which lead to oscillations in the vicinity of discontinuities. We apply well-known SBP-SAT compatible numerical diffusion operators in case of discontinuous data.

The rest of this paper is organized as follows: In Section 2.2, we state the energy estimate for the initial-boundary value problem corresponding to (2.1.4) in order to motivate the proof of stability for the scheme. In Section 2.3, we present the SBP-SAT scheme and show stability. Numerical experiments are presented in Section 2.4 and conclusions are

drawn in Section 2.5.

2.2 The Continuous problem

For ease of notation, we shall restrict ourselves to two spatial dimensions in the remainder of this paper. Extending the results to three dimensions is straightforward.

In two dimensions, the non-conservative symmetric form (2.1.4) reads

$$\mathbf{B}_t + \Lambda_1 \mathbf{B}_x + \Lambda_2 \mathbf{B}_y - C\mathbf{B} = 0, \tag{2.2.1}$$

where

$$\Lambda_1 = \begin{pmatrix} u^1 & 0 \\ 0 & u^1 \end{pmatrix}, \quad \Lambda_2 = \begin{pmatrix} u^2 & 0 \\ 0 & u^2 \end{pmatrix}, \quad C = \begin{pmatrix} -\partial_y u^2 & \partial_y u^1 \\ \partial_x u^2 & -\partial_x u^1 \end{pmatrix},$$

with $\mathbf{B} = (B^1, B^2)^T$ and $\mathbf{u} = (u^1, u^2)^T$ denoting the magnetic and velocity fields respectively. In component form, (2.2.1) becomes

$$\begin{aligned} (B^1)_t + u^1(B^1)_x + u^2(B^1)_y &= -(u^2)_y B^1 + (u^1)_y B^2 \\ (B^2)_t + u^1(B^2)_x + u^2(B^2)_y &= (u^2)_x B^1 - (u^1)_x B^2. \end{aligned} \tag{2.2.2}$$

To begin with, we shall consider (2.2.1) in the domain $(x, y) \in \Omega = [0, 1]^2$.

We augment (2.2.1) with initial conditions,

$$\mathbf{B}(\mathbf{x}, 0) = \mathbf{B}_0(\mathbf{x}) \quad \mathbf{x} \in \Omega, \tag{2.2.3}$$

and Dirichlet boundary conditions,

$$\begin{aligned} &\mathbf{1}_{\{u^1(0,y,t)>0\}}\Big(\mathbf{B}(0,y,t) = \mathbf{g}(0,y,t)\Big), \quad \mathbf{1}_{\{u^1(1,y,t)<0\}}\Big(\mathbf{B}(1,y,t) = \mathbf{g}(1,y,t)\Big), \\ &\mathbf{1}_{\{u^2(x,0,t)>0\}}\Big(\mathbf{B}(x,0,t) = \mathbf{g}(x,0,t)\Big), \quad \mathbf{1}_{\{u^2(x,1,t)<0\}}\Big(\mathbf{B}(x,1,t) = \mathbf{g}(x,1,t)\Big) \end{aligned} \tag{2.2.4}$$

where $\mathbf{1}_A$ denotes the characteristic function of the set A. Note that we only impose boundary conditions on the set where the characteristics are entering the domain.

Definition 2.2.1. *Weak solution: A function $\mathbf{B} : \Omega \to \mathbb{R}^2$ such that $\mathbf{B} \in C([0, T]; H^1(\Omega))$ is defined as a weak solution of (2.2.1) with initial data (2.2.3) and boundary data (2.2.4) if it satisfies the weak formulation of (2.2.1) in Ω, i.e.,*

$$\begin{aligned} &\int_0^T \int_\Omega \mathbf{B} \left(\varphi_t + (\Lambda_1 \varphi)_x + (\Lambda_2 \varphi)_y - C\varphi\right) dxdydt + \int_\Omega \mathbf{B}_0 \varphi(x, y, 0)\, dxdy \\ &\quad - \int_0^T \int_0^1 u^1 \left(Tr\mathbf{B}\right) \varphi(x, y, t) \Big|_{x=0}^{x=1} dydt - \int_0^T \int_0^1 u^2 \left(Tr\mathbf{B}\right) \varphi(x, y, t) \Big|_{y=0}^{y=1} dxdt = 0, \end{aligned} \tag{2.2.5}$$

for all test functions $\varphi \in C_0^\infty(\Omega \times [0, T))$. By $Tr\mathbf{B}$ we mean the H^1 trace of $\mathbf{B}$ at the boundary. The boundary conditions (2.2.4) are taken in the sense of H^1 traces.

We shall always assume that the initial and boundary data satisfy the compatibility conditions, i.e., specific criteria that guarantee smoothness of the solution, see [9].

Theorem 2.2.1. *Assume that* $\mathbf{B}_0 \in H^1(\Omega)$, *that* $\mathbf{g} \in H^1(\partial\Omega \times [0,T])$ *for* $T > 0$ *and that* u^1 *and* u^2 *are in* $H^2(\Omega \times [0,T])$. *Then there exists a function* $\mathbf{B} \in C([0,T], L^2(\Omega)) \cap L^\infty([0,T]; H^1(\Omega))$ *which is the unique weak solution of (2.2.1) with the initial and boundary conditions (2.2.3) and (2.2.4).*

Furthermore, it satisfies the following stability estimate

$$\|\mathbf{B}(\cdot,t)\|^2_{H^1(\Omega)} \leq e^{\alpha t}\left(\|\mathbf{B}_0\|^2_{H^1(\Omega)} + \|\mathbf{g}\|_{H^1(\partial\Omega\times(0,t))}\right). \tag{2.2.6}$$

where α *is a positive constant.*

Proof. The proof of this theorem is standard. Assume first that $\mathbf{g}$, $\mathbf{B}_0$ and $\mathbf{u}$ are in C^∞. Since the compatibility conditions are satisfied, a unique solution exists by the method of characteristics. Let $(a \vee 0) = \max\{a, 0\}$ and $(a \wedge 0) = \min\{a, 0\}$. Multiplying the equation by $\mathbf{B}$ and integrating over Ω yields

$$\begin{aligned}
&\frac{d}{dt}\int_\Omega \mathbf{B}^T\mathbf{B}\,dxdy \\
&= \int_\Omega \mathbf{B}\left(2C + \operatorname{div}(\mathbf{u})\right)\mathbf{B}\,dxdy - \int_0^1 u^1 Tr(\mathbf{B}^T\mathbf{B})\,\big|_{x=0}^{x=1}\,dy + \int_0^1 u^2 Tr(\mathbf{B}^T\mathbf{B})\,\big|_{y=0}^{y=1}\,dx \\
&\leq c\int_\Omega \mathbf{B}^T\mathbf{B}\,dxdy \\
&\quad + \int_0^1 \left(u^1(0,y,t)\vee 0\right)\left(Tr(\mathbf{B}^T\mathbf{B})\right)\,dy - \int_0^1 \left(u^1(1,y,t)\wedge 0\right)\left(Tr(\mathbf{B}^T\mathbf{B})\right)\,dy \\
&\quad + \int_0^1 \left(u^2(x,0,t)\vee 0\right)\left(Tr(\mathbf{B}^T\mathbf{B})\right)\,dx - \int_0^1 \left(u^2(x,1,t)\wedge 0\right)\left(Tr(\mathbf{B}^T\mathbf{B})\right)\,dx \\
&\leq c\left(\int_\Omega (\mathbf{B}^T\mathbf{B})\,dxdy + \int_{\partial\Omega}\mathbf{g}^2\,ds\right)
\end{aligned}$$

for some constant c depending on $\mathbf{u}$ and its first derivatives. Via the Grönwall inequality we get the bound

$$\|\mathbf{B}(\cdot,t)\|^2_{L^2(\Omega)} \leq e^{ct}\left(\|\mathbf{B}_0\|^2_{L^2(\Omega)} + \int_0^T\int_{\partial\Omega}\mathbf{g}^2\,ds\,dt\right).$$

Set $\mathbf{P} = \mathbf{B}_x$ and $\mathbf{Q} = \mathbf{B}_y$, applying ∂_x to (2.2.1) yields

$$\mathbf{P}_t + u^1\mathbf{P}_x + u^2\mathbf{P}_y = u^1_x\mathbf{P} + u^2_x\mathbf{Q} + C\mathbf{P} + C_x\mathbf{B}. \tag{2.2.7}$$

Furthermore, $P(x,y,0) = \partial_x\mathbf{B}_0(x,y)$ and at those parts of $\partial\Omega$ where we impose data

$$\begin{aligned}
u^1\mathbf{P} &= C\mathbf{g} - \mathbf{g}_t - u^2\mathbf{g}_y \quad \text{on } x = 0 \text{ and } x = 1, \\
u^2\mathbf{Q} &= C\mathbf{g} - \mathbf{g}_t - u^2\mathbf{g}_x \quad \text{on } y = 0 \text{ and } y = 1.
\end{aligned}$$

We shall also be needing $\mathbf{P}$ on $y = 0$ and 1 and $\mathbf{Q}$ on $x = 0$ and 1. These are given by $\mathbf{g}_x$ and $\mathbf{g}_y$ respectively.

Multiplying (2.2.7) with $2\mathbf{P}^T$ and rearranging yields

$$\mathbf{P}_t^2 + \left(u^1\mathbf{P}^2\right)_x + \left(u^2\mathbf{P}^2\right)_y = -u_x^1\mathbf{P}^2 - 2u_x^2\mathbf{P}^T\mathbf{Q} + 2\mathbf{P}^T C\mathbf{P} + 2\mathbf{P}^T C_x\mathbf{B}.$$

We also have an analogous equation for $\mathbf{Q}^2$;

$$\mathbf{Q}_t^2 + \left(u^1\mathbf{Q}^2\right)_x + \left(u^2\mathbf{Q}^2\right)_y = -u_y^2\mathbf{Q}^2 - 2u_y^1\mathbf{P}^T\mathbf{Q} + 2\mathbf{P}^T C\mathbf{Q} + 2\mathbf{Q}^T C_y\mathbf{B}.$$

Adding these two equations we find

$$\left(\mathbf{P}^2 + \mathbf{Q}^2\right)_t + \left(u^1\left(\mathbf{P}^2 + \mathbf{Q}^2\right)\right)_x + \left(u^2\left(\mathbf{P}^2 + \mathbf{Q}^2\right)\right)_y = R, \tag{2.2.8}$$

where by Hölder's inequality R has the bound

$$\int_\Omega R(x,y,t)\,dxdy \le c\left(\|\mathbf{B}(\cdot,t)\|_{L^2(\Omega)}^2 + \|\mathbf{P}(\cdot,t)\|_{L^2(\Omega)}^2 + \|\mathbf{Q}(\cdot,t)\|_{L^2(\Omega)}^2\right),$$

where the constant c depends on $\mathbf{u}$ and its derivatives. By reasoning as we did with $\mathbf{B}$, we can then get the bound

$$\frac{d}{dt}\left(\|\mathbf{P}\|_{L^2(\Omega)}^2 + \|\mathbf{Q}\|_{L^2(\Omega)}^2\right) \le c\left(\|\mathbf{B}(\cdot,t)\|_{L^2(\Omega)}^2 + \|\mathbf{P}\|_{L^2(\Omega)}^2 + \|\mathbf{Q}\|_{L^2(\Omega)}^2 + \int_{\partial\Omega}\mathbf{g}_t^2 + \mathbf{g}_x^2 + \mathbf{g}_y^2\,ds\right).$$

Via Grönwall's inequality and the bounds on $\|\mathbf{B}\|_{L^2}$ we find

$$\|\mathbf{P}(\cdot,t)\|_{L^2(\Omega)}^2 + \|\mathbf{Q}(\cdot,t)\|_{L^2(\Omega)}^2 \le \text{Const.},$$

where the constant depends on the $H^1(\Omega)$ norm of $\mathbf{B}_0$ and $\mathbf{g}$ and on $\mathbf{u}$ and its derivatives. This means that we have an energy estimate

$$\|\mathbf{B}(\cdot,t)\|_{H^1(\Omega)} \le C_t\left(\|\mathbf{B}_0\|_{H^1(\Omega)} + \|\mathbf{g}\|_{H^1(\partial\Omega\times(0,t))}\right),$$

where C_t is a finite constant depending on t, $\mathbf{u}$ and its derivatives.

Then, for a general initial data, velocity fields and boundary conditions, we can use a standard approximation argument ([10]) and the above estimate to pass to the limit and prove the existence and uniqueness of weak solutions. □

Remark 2.2.1. *The above theorem has been proved in the unit square. It can be easily extended to domains with smooth (i.e., C^1 boundaries) by using cut-off functions and mappings between the domain and the upper-half space. See [19] and other references therein for details.*

2.3 Semi-discrete Schemes

As stated before, we will approximate (2.2.1) with SBP-SAT finite difference schemes. We start by defining a SBP operator approximating the first derivative of a continuous function $w(x)$ in one space dimension. Let $\{x_i\}_{i=0}^n$ be equidistant points in $[0,1]$ such that $x_i = ih$ where $h = 1/n$. We organize the values of w at $\{x_i\}$ in a vector $w^T(t) = (w_0, ..., w_n)$ where $w_i = w(x_i)$. Then , we define,

Definition 2.3.1. *A difference approximation (given by a $(n+1)\times(n+1)$ matrix D) for the first derivative is called a* Summation-By-Parts *(SBP) operator if $D = P^{-1}Q$ for $n\times n$ matrices P and Q, where $P > 0$, $P = P^T$ and $Q + Q^T = \mathcal{B} = \mathrm{diag}(-1, 0, 0, \ldots, 0, 0, 1)$.*

Moreover, P must define a scalar product $(w, v) = w^T P v$ for which the corresponding norm, $\|w\|_P^2 = (w, w)$, is equivalent to the standard l^2-norm, $\|w\|_2^2 = h\sum_{i=1}^n w_i^2$.

SBP operators of different orders of accuracy are presented in several papers, see the references in e.g. [22]. To discretize (2.2.1), we introduce equidistant meshes in the x and y directions with N and M mesh points and $\Delta x = 1/N$ and $\Delta y = 1/M$. The discrete solution consists of a column vector of length $2(N+1)(M+1)$ denoted $V = (V^1, V^2)^T$, where V^ℓ is a vector of length $(N+1)(M+1)$ ordered as

$$V^\ell = \left(V_{0,0}^\ell, V_{0,1}^\ell, \ldots, V_{0,N}^\ell, V_{1,0}^\ell, \ldots, \ldots, V_{N,M}^\ell\right).$$

and $V_{i,j}^\ell$ is the discrete solution at (x_i, y_j) for $\ell = 1, 2$. We will use the norm

$$\|w\|_P^2 = w^T(P_x \otimes P_y)w$$

where we have introduced the Kronecker product, which is defined as follows:

Let A and C be $n \times n$ matrices and B and D be $m \times m$ matrices. Then $A \otimes B$ is the $nm \times nm$ matrix

$$(A \otimes B) = \begin{pmatrix} a_{11}B & \ldots & a_{1n}B \\ \vdots & \ddots & \vdots \\ a_{n1}B & \ldots & a_{nn}B \end{pmatrix}.$$

Furthermore, the following rules hold; $(A\otimes B)(C\otimes D) = (AC\otimes BD)$, $(A\otimes B)+(C\otimes D) = (A + C) \otimes (B + D)$ and $(A \otimes B)^T = (A^T \otimes B^T)$.

To define discrete boundary conditions, we need some further notation. For real numbers σ_i, introduce the 2×2 matrices

$$\Sigma_{0,y} = \sigma_1 I_2, \quad \Sigma_{N,y} = \sigma_2 I_2, \quad \Sigma_{x,0} = \sigma_3 I_2, \quad \Sigma_{x,N} = \sigma_4 I_2,$$

where the I_2 is the 2×2 identity matrix and the numbers σ_i are to be determined later. We also need $(M + 1) \times (M + 1)$ matrices $F_{0,y}$ and $F_{N,y}$

$$F_{0,y} = \begin{pmatrix} 1 & 0 & \cdot & \cdot & \cdot & 0 \\ 0 & \cdot & \cdot & \cdot & \cdot & 0 \\ \cdot & \cdot & \cdot & \cdot & \cdot & \cdot \\ 1 & 0 & \cdot & \cdot & \cdot & 0 \\ 0 & \cdot & \cdot & \cdot & \cdot & 0 \\ \cdot & \cdot & \cdot & \cdot & \cdot & \cdot \end{pmatrix}, \quad F_{N,y} = \begin{pmatrix} 0 & \cdot & \cdot & \cdot & \cdot & 1 \\ 0 & \cdot & \cdot & \cdot & \cdot & 0 \\ \cdot & \cdot & \cdot & \cdot & \cdot & \cdot \\ 0 & \cdot & \cdot & \cdot & \cdot & 1 \\ 0 & \cdot & \cdot & \cdot & \cdot & 0 \\ \cdot & \cdot & \cdot & \cdot & \cdot & \cdot \end{pmatrix},$$

and $(N+1)\times(N+1)$ matrices $F_{x,0}$ and $F_{x,M}$,

$$F_{x,0} = \begin{pmatrix} 1 & 0 & \cdot & \cdot & \cdot & 0 \\ 0 & \cdot & \cdot & \cdot & \cdot & 0 \\ \cdot & \cdot & \cdot & \cdot & \cdot & \cdot \\ 1 & 0 & \cdot & \cdot & \cdot & 0 \\ 0 & \cdot & \cdot & \cdot & \cdot & 0 \\ \cdot & \cdot & \cdot & \cdot & \cdot & \cdot \end{pmatrix}, \quad F_{x,M} = \begin{pmatrix} 0 & \cdot & \cdot & \cdot & \cdot & 1 \\ 0 & \cdot & \cdot & \cdot & \cdot & 0 \\ \cdot & \cdot & \cdot & \cdot & \cdot & \cdot \\ 0 & \cdot & \cdot & \cdot & \cdot & 1 \\ 0 & \cdot & \cdot & \cdot & \cdot & 0 \\ \cdot & \cdot & \cdot & \cdot & \cdot & \cdot \end{pmatrix}.$$

Next set

$$E_{0,y} = I_x \otimes F_{0,y}, \quad E_{N,y} = I_x \otimes F_{N,y}, \quad E_{x0} = F_{x,0} \otimes I_y, \quad \text{and} \quad E_{x,M} = F_{x,M} \otimes I_y$$

where I_x and I_y are $(N+1)\times(N+1)$ and $(M+1)\times(M+1)$ identity matrices respectively and define

$$\begin{aligned} \Lambda_x &= I_2 \otimes \operatorname{diag}\left(u^1_{0,0}, u^1_{0,1}, \ldots, u^1_{0,N}, u^1_{1,0}, \ldots, \ldots, u^1_{N,M}\right) \\ \Lambda_y &= I_2 \otimes \operatorname{diag}\left(u^2_{0,0}, u^2_{0,1}, \ldots, u^2_{0,N}, u^2_{1,0}, \ldots, \ldots, u^2_{N,M}\right). \end{aligned}$$

Define the matrix C by,

$$C = \begin{pmatrix} -\left(I_x \otimes \left(P_y^{-1}Q_y\right)\right) u^2 & \left(I_x \otimes \left(P_y^{-1}Q_y\right)\right) u^1 \\ \left(\left(P_x^{-1}Q_x\right) \otimes I_y\right) u^2 & -\left(\left(P_x^{-1}Q_x\right) \otimes I_y\right) u^1 \end{pmatrix}.$$

Let g be a column vector of the same length as V, where we store the boundary values at the appropriate places. Then we can describe the SBP-SAT scheme as

$$\begin{aligned} &\partial_t V + \Lambda_x \left(I_2 \otimes \left(P_x^{-1}Q_x\right) \otimes I_y\right) V + \Lambda_y \left(I_2 \otimes I_x \otimes \left(P_y^{-1}Q_y\right)\right) V + CV \\ &\quad = \Sigma_{0,y} \otimes \left(P_x^{-1} \otimes I_y\right) \otimes E_{0y}\left(V - g\right) + \Sigma_{Ny} \otimes \left(P_x^{-1} \otimes I_y\right) \otimes E_{N,y}\left(V - g\right) \\ &\qquad + \Sigma_{x0} \otimes \left(I_x \otimes P_y^{-1}\right) \otimes E_{x0}\left(V - g\right) + \Sigma_{x,N} \otimes \left(I_x \otimes P_y^{-1}\right) \otimes E_{xN}\left(V - g\right), \end{aligned} \tag{2.3.1}$$

Theorem 2.3.1. *Assume that the velocity field* $\mathbf{u}$ *is a constant given by* $\mathbf{u} = (u^1, u^2)^T$, *and let* V *be the semi-discrete solution defined by the scheme (2.3.1). Let* $u^{\ell,+} = \left(u^\ell \vee 0\right)$ *and* $u^{\ell,-} = \left(u^\ell \wedge 0\right)$, *for* $\ell = 1, 2$. *If the penalty parameters satisfy*

$$\sigma_1 \leq -\frac{u^{1,+}}{2}, \ \sigma_2 \leq -\frac{u^{1,-}}{2}, \ \sigma_3 \leq \frac{u^{2,+}}{2} \quad \text{and} \quad \sigma_4 \leq \frac{u^{2,-}}{2} \tag{2.3.2}$$

there exists positive constants α *and* K *such that*

$$\|V(t)\|^2 \leq \|\mathbf{B}_0\|^2 + \int_0^t \int_{\partial\Omega} \mathbf{g}(t,x)\, dx d\tau, \tag{2.3.3}$$

and the scheme (2.3.1) is stable.

Proof. The proof is similar to the standard way of proving stability of SBP-SAT schemes (see [22]) and follows the proof for obtaining energy stability of the continuous problem in theorem 2.2.1. We outline the proof for the sake of completeness. For simplicity, we consider the case of constant velocities by setting $C = 0$ in (2.3.1) We start by multiplying (2.3.1) with $V^T(I_2 \otimes P_x \otimes P_y)$ to obtain,

$$\begin{aligned} &V^T \left(I_2 \otimes P_x \otimes P_y\right) \partial_t V \\ &\quad = -V^T \left(\Lambda_x \otimes Q_x \otimes P_y\right) V + V^T \left(\Lambda_y \otimes P_x \otimes Q_y\right) V \\ &\qquad + V^T (I_2 \otimes P_x \otimes P_y) \otimes \begin{bmatrix} \left(\Sigma_{0y} \otimes P_x^{-1} \otimes I_y\right) E_{0,y} + \left(\Sigma_{N,y} \otimes P_x^{-1} \otimes I_y\right) E_{N,y} \\ + (\Sigma_{x,0} \otimes I_x \otimes P_y^{-1}) E_{x,0} + (\Sigma_{x,N} \otimes I_x \otimes P_y^{-1}) E_{x,M} \end{bmatrix} V. \end{aligned} \tag{2.3.4}$$

Adding this to its transpose and using the definition of SBP operators, we obtain

$$\begin{aligned} &\frac{d}{dt} \|V\|^2 \\ &\quad = -V^T \left(\Lambda_1 \otimes \mathcal{B}_x \otimes P_y\right) V + V^T \left(\Lambda_2 \otimes P_x \otimes \mathcal{B}_y\right) V \\ &\qquad + 2V^T (I_2 \otimes P_x \otimes P_y) \otimes \begin{bmatrix} \left(\Sigma_{0,y} \otimes P_x^{-1} \otimes I_y\right) E_{0,y} + \left(\Sigma_{N,y} \otimes P_x^{-1} \otimes I_y\right) E_{N,y} \\ + \left(\Sigma_{x,0} \otimes I_x \otimes P_y^{-1}\right) E_{x,0} + \left(\Sigma_{x,N} \otimes I_x \otimes P_y^{-1}\right) E_{x,N} \end{bmatrix} V, \end{aligned}$$

which implies

$$\begin{aligned} \frac{d}{dt} \|V\|^2 = {} & u^1 \left(V^1_{0,y}\right)^T P_y \left(V^1_{0,y}\right) - u^1 \left(V^1_{N,y}\right)^T P_y \left(V^1_{N,y}\right) + u^1 \left(V^2_{0,y}\right)^T P_y \left(V^2_{0,y}\right) \\ & - u^1 \left(V^2_{N,y}\right)^T P_y \left(V^2_{N,y}\right) + u^2 \left(V^1_{x,0}\right)^T P_x \left(V^1_{x,0}\right) - u^2 \left(V^1_{x,M}\right)^T P_x \left(V^1_{x,M}\right) \\ & + u^2 \left(V^2_{x,0}\right)^T P_x \left(V^2_{x,0}\right) - u^2 \left(V^2_{x,N}\right)^T P_x \left(V^2_{x,N}\right) \\ & + 2\Big[\sigma_1 \left(\left(V^1_{0,y}\right)^T P_y \left(V^1_{0y}\right) + \left(V^2_{0,y}\right)^T P_y \left(V^2_{0,y}\right)\right) + \sigma_2 \left(V^1_{N,y}\right)^T P_y \left(V^1_{N,y}\right) \\ & \qquad + \sigma_2 \left(V^2_{N,y}\right)^T P_y \left(V^2_{N,y}\right) + \sigma_3 \left(\left(V^1_{x,0}\right)^T P_x \left(V^1_{x,0}\right) + \left(V^2_{x,0}\right)^T P_x \left(V^2_{x,0}\right)\right) \\ & \qquad + \sigma_4 \left(\left(V^1_{x,N}\right)^T P_x \left(V^1_{x,N}\right) \left(V^2_{x,N}\right)^T P_x \left(V^2_{x,N}\right)\right)\Big]. \end{aligned}$$

Using (2.3.2) and integrating in time gives the energy estimate (2.3.3). □

Remark 2.3.1. *The above proof of stability assumes a constant velocity field. A proof of stability with a general velocity fields has been obtained in a recent paper [8] by using the principle of frozen coefficients. The resulting stability estimate will lead to an exponential growth of energy (similar to (2.2.6)) due to the presence of lower order terms.*

We conclude this section with a few comments. For simplicity, we have only considered Cartesian meshes. However, the proofs are readily generalized to curvilinear grids by transforming the domain to a Cartesian. A stability proof is then obtained by freezing the coefficients. However, that requires P to be diagonal, [21]. Furthermore, multi-block grids can also be handled and stable interfaces derived in a similar way as in, [16].

2.4 Numerical Experiments

We test the SBP-SAT schemes of the previous section on a suite of numerical experiments in order to demonstrate the effectiveness of these schemes. We will use two different schemes : $SBP2$ and $SBP4$ scheme which are second-order (first-order) and fourth order (second-order) accurate in the interior (boundary) resulting in an overall second and third-order of accuracy. Time integration is performed by using a second order accurate Runge-Kutta scheme at a CFL number of 0.45 for all numerical experiments. We found that using a fourth order accurate Runge-Kutta scheme resulted in negligible differences in the numerical results. The schemes have bounded errors, a typical behavior for hyperbolic equations with characteristic boundary conditions as shown in [15]. Errors are propagated through the domain and leave the domain on account of the transparent boundaries. Hence, errors do not accumulate in time. On small domains, spatial errors become dominant.

Numerical experiment 1: In this experiment, we consider (2.2.1) with the divergence-free velocity field $\mathbf{u}(x, y) = (-y, x)^T$. The exact solution can be easily calculated by the method of characteristics and takes the form

$$\mathbf{B}(\mathbf{x}, t) = R(t)\mathbf{B}_0(R(-t)\mathbf{x}), \tag{2.4.1}$$

where $R(t)$ is a rotation matrix with angle t and represents rotation of the initial data about the origin.

We consider the same test setup as in [11] and [5] by choosing the divergence free initial data,

$$\mathbf{B}_0(x, y) = 4 \begin{pmatrix} -y \\ x - \frac{1}{2} \end{pmatrix} e^{-20\left((x-1/2)^2+y^2\right)}, \tag{2.4.2}$$

and the computational domain $[-1, 1] \times [-1, 1]$. Since the exact solution is known in this case, one can in principle use this to specify the boundary data g. Instead, we decided to mimic a free space boundary (artificial boundary) by taking $g = 0$. (which is a good guess at a far-field boundary).

We run this test case with $SBP2$ and $SBP4$ schemes and present different sets of results. In Figure 2.4.1, we plot $|\mathbf{B}| = (|B^1|^2 + |B^2|^2)^{1/2}$ at times $t = \pi$ (half-rotation) and $t = 2\pi$ (one full rotation) with the $SBP2$ and $SBP4$ schemes. As shown in this figure, $SBP2$ and $SBP4$ schemes resolve the solution quite well. In fact, $SBP4$ is very accurate and keeps the hump intact throughout the rotation. In Table 2.4.1, we present percentage relative errors in l^2. The errors are computed at time $t = 2\pi$ (one rotation) on a sequence of meshes for both the $SBP2$ and $SBP4$ schemes. The results show that the errors are quite low, particularly for $SBP4$ and the rate of convergence approaches the expected values of 2 for $SBP2$ and 3 for $SBP4$. Furthermore, the order of accuracy is unaffected at these resolutions by using zero Dirichlet boundary data instead of the exact solution at the boundary.

In order to compare the SBP schemes of this paper with other existing schemes, we choose to compute the solutions for this problem with both the first- and the second-order divergence-preserving scheme of [11], which we label as the TF and $TF2$ schemes. Furthermore, we compute the solutions using the first order stable upwind scheme designed

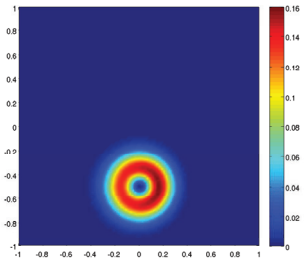

(a) half rotation, SBP2

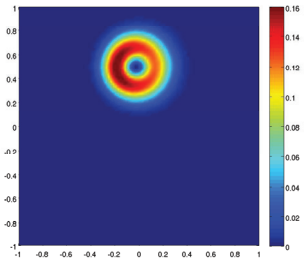

(b) full rotation, SBP2

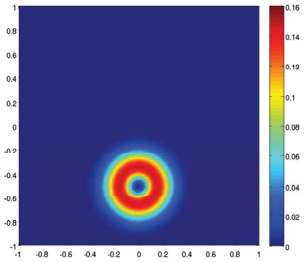

(c) half rotation, SBP4

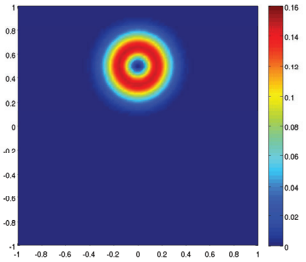

(d) full rotation, SBP4

Figure 2.4.1: Numerical results for $|\mathbf{B}|$ in experiment 1.

Grid size	$SBP2$	rate	$SBP4$	rate
40×40	6.9×10^{1}		8.0×10^{0}	
80×80	2.1×10^{1}	1.7	5.0×10^{-1}	4.0
160×160	5.5×10^{0}	2.0	4.5×10^{-2}	3.5
320×320	1.3×10^{0}	2.0	5.1×10^{-3}	3.1
640×640	3.3×10^{-1}	2.0	6.4×10^{-4}	3.0

Table 2.4.1: Relative percentage errors in l^2 for $|\mathbf{B}|$ at time $t = 2\pi$ and rates of convergence for numerical experiment 1 with $SBP2$ and $SBP4$ schemes.

in [5], labeled the SUS scheme. The relative errors with each of these schemes are shown in Table 2.4.2. Results in Tables 2.4.1 and 2.4.2 show that the TF and SUS schemes

Grid size	SUS	TF	$TF2$
40×40	8.6×10^1	7.6×10^1	1.8×10^1
80×80	7.3×10^1	6.4×10^1	1.3×10^1
160×160	5.4×10^1	4.7×10^1	3.0×10^0
320×320	3.6×10^1	3.3×10^1	1.0×10^0
640×640	2.0×10^1	1.4×10^1	2.7×10^{-1}

Table 2.4.2: Relative percentage errors in l^2 for $|\mathbf{B}|$ at $t = 2\pi$ and for numerical experiment 1 with the SUS, TF, $TF2$, $SBP2$ and the $SBP4$ schemes.

lead to similar errors and these errors are considerably larger than the errors generated by the $TF2$ and $SBP2$ schemes, while the errors generated by the $SBP4$ scheme are much smaller again.

A fair comparison of the the five schemes SUS, TF, TF2, SBP2 and SBP4 requires information on the computational work with each scheme for the same error level. We observe from tables 2.4.1 and 2.4.2 that for a given relative error of approximately 20 percent, the first-order SUS scheme requires a 640×640 mesh, the TF scheme requires a 500×500 mesh (based on extrapolation from table 2.4.2), whereas both the second-order schemes require meshes coarser than a 50×50 mesh. The fourth-order scheme yields similar error levels on even coarser meshes. Thus, the second-order schemes require about 1% of the total grid points to the first-order schemes to produce comparable errors. Even taking into account that the second order schemes use more operations for each grid point, this still makes the second order schemes at least $25 - 30$ times more efficient than the first order schemes. Similarly an error level of about one percent is attained with SBP2 on a 320×320 mesh, with TF2 on a similar 320×320 mesh and with SBP4 on a 50×50 mesh. Thus the second order schemes need about 36 times more grid points to produce errors similar to those of the fourth order schemes. Taking extra work for the fourth-order scheme per grid point into account, we still get that the fourth-order scheme is roughly 10 times more efficient than the second-order schemes. These numbers are approximations but display a clear qualitative trend i.e., it is much more efficient to use high-order schemes for the induction equations.

As the solution (2.4.1) in this case is smooth, it is also a solution for the constrained form (2.1.3). Furthermore, the initial data is divergence free and so is the exact solution. We did not attempt to preserve any particular form of discrete divergence while designing the SBP schemes (2.3.1). A natural thing would be show that some form of discrete divergence produced by the schemes was bounded in l^2. We were unable to obtain such a divergence bound for (2.3.1) in this paper. A related SBP-SAT scheme for the "conservative" symmetric form (2.1.5) with SBP operators for discretizing spatial derivatives coupled with a novel discretization of the source terms in (2.1.5) was shown to have bounded discrete divergence in a recent paper [8].

In the absence of a rigorous divergence bound, we proceed to examine how divergence errors generated by the SBP schemes behave and whether they have any impact on the

quality of the discretization. We define the following discrete divergence,

$$\mathrm{div}_P(V) = (P_x^{-1}Q_x \otimes I_y)V^1 + (I_x \otimes P_y^{-1}Q_y)V^2.$$

This corresponds to the standard centered discrete divergence operator at the corresponding order of accuracy. The divergence errors in l^2 and rates of convergence at time $t = 2\pi$ for the $SBP2$ and $SBP4$ schemes on a sequence of meshes are presented in Table 2.4.3. From Table 2.4.3, we conclude that although the initial divergence is zero, the discrete

Grid size	$SBP2$	rate	$SBP4$	rate
20×20	1.0×10^{0}		7.3×10^{-1}	
40×40	8.0×10^{-1}	0.4	1.2×10^{-1}	2.6
80×80	2.7×10^{-1}	1.6	8.2×10^{-3}	3.8
160×160	7.0×10^{-2}	2.0	1.0×10^{-3}	3.0
320×320	2.5×10^{-2}	1.5	1.7×10^{-4}	2.6

Table 2.4.3: Numerical Experiment 1: Divergence (errors) in l^2 and rates of convergence at time $t = 2\pi$ for both the $SBP2$ and $SBP4$ schemes.

divergence computed with both the $SBP2$ and $SBP4$ schemes is not zero. However, the divergence errors are very small even on fairly coarse meshes and converge to zero at a rate of 1.5 and 2.5 for $SBP2$ and $SBP4$ schemes respectively. A simple truncation error analysis suggests that these rates for the $SBP2$ and $SBP4$ schemes are optimal. The quality of the approximations is good and the rates of convergence do not seem to suffer from not preserving any form of discrete divergence.

In order to compare with existing schemes, we compare the divergence errors generated by the SUS, TF and the $TF2$ schemes with the $SBP2$ and the $SBP4$ schemes in table 2.4.4. From Table 2.4.4, we can draw the following conclusions about divergence

Grid size	SUS	TF	$TF2$
40×40	1.1×10^{-1}	2.7×10^{-2}	1.2×10^{-2}
80×80	1.3×10^{-1}	1.7×10^{-2}	4.0×10^{-3}
160×160	1.4×10^{-1}	1.4×10^{-2}	2.4×10^{-3}
320×320	1.1×10^{-1}	1.2×10^{-2}	9.7×10^{-4}

Table 2.4.4: Numerical Experiment 1: The discrete divergence div_P in l^2 at $t = 2\pi$ for the SUS, TF and $TF2$ schemes.

errors. The SUS scheme is not tailored to preserve any form of discrete divergence. The divergence errors generated by this scheme seems to be low on coarse meshes. The TF and $TF2$ schemes are designed to preserve a special form of discrete divergence which is different from the standard central form. Nevertheless, the analysis presented in [11] suggested that the errors in the standard divergence operator will also be quite low. This is indeed the case. On the coarser meshes, the divergence is much larger for the $SBP2$ scheme than the TF schemes, but from Table 2.4.2 we see that the errors in the solution are similar.

Furthermore, the divergence errors converge quickly for the $SBP4$ scheme, as well as as the for the $TF2$ scheme. The above results indicate that controlling some form of discrete divergence is not necessary to approximate solutions of the magnetic induction equations in a stable and accurate manner.

Next, we consider long time integration. The energy estimate (2.3.3) suggests that the energy of the approximate solutions can grow exponentially in time. In order to test this we computed approximate solutions with the $SBP2$, $SBP4$ and the $TF2$ schemes till time $t = 100\pi$, i.e., for fifty full rotations on a 100×100 mesh. The numerical results in are presented in Figure 2.4.2 and Table 2.4.5. These computations were performed

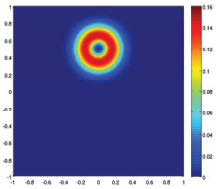

(a) $t = 0$

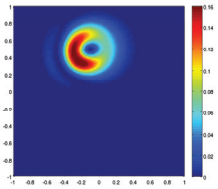

(b) $t = 10\pi$, SBP2

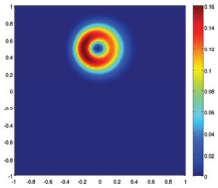

(c) $t = 100\pi$, SBP4

Figure 2.4.2: Numerical results for $|\mathbf{B}|$ in experiment 1.

on a fixed 100×100 mesh. In Figure 2.4.2, we compare the $SBP2$ and $SBP4$ schemes after five and fifty rotations respectively. We see that after 5 rotations, $SBP2$ gives a "hump" which is somewhat smeared and with a pronounced asymmetry. On the other hand, the hump produced by the $SBP4$ scheme is much more accurate. As shown in Table 2.4.5, the absolute errors with the $SBP4$ scheme are much lower than the errors due to the second-order schemes $SBP2$ and $TF2$. In fact, the errors with $SBP2$ after just five rotations are about three times the error with $SBP4$ after fifty rotations. This experiment makes a strong case for using high-order schemes for problems requiring long time integration.

Numerical Experiment 2: In the previous numerical experiment, the hump was confined to the interior of the domain during the rotation. Hence, the choice of zero Dirichlet

$2\pi t$	$SBP2$	$SBP4$	$TF2$
$t=1$	2.1×10^{1}	5.1×10^{-1}	8.8×10^{0}
$t=5$	7.7×10^{1}	2.7×10^{0}	3.2×10^{1}
$t=10$	1.0×10^{2}	4.7×10^{0}	5.0×10^{1}
$t=15$	1.1×10^{2}	6.6×10^{0}	6.3×10^{1}
$t=20$	1.2×10^{2}	8.7×10^{0}	7.2×10^{1}
$t=30$	1.2×10^{2}	1.9×10^{1}	8.4×10^{1}
$t=40$	1.3×10^{2}	3.1×10^{1}	9.2×10^{1}
$t=50$	1.4×10^{2}	4.3×10^{1}	1.0×10^{2}

Table 2.4.5: Relative percentage l^2 errors in $|\mathbf{B}|$ with $SBP2$, $SBP4$ and $TF2$ for numerical experiment 1.

data at the boundary was reasonable and led to stable and accurate approximations. In order to illustrate the effect of the boundary better, we choose the computational domain $[0,1]\times[0,1]$ and use the same velocity field and initial data as in the previous experiment. Now, the hump "exits" the domain at one part of the boundary (including a corner) and will re-enter the domain from another part of the boundary. The choice of boundary discretization becomes crucial in this case.

We select the exact solution (2.4.1) restricted to the boundary as the Dirichlet boundary data in (2.3.1). In Figure 2.4.3, the approximate solutions computed with both $SBP2$ and $SBP4$ on a 100×100 mesh are plotted at time $t=\pi/2$ (quarter rotation) and time $t=2\pi$ (full rotation). As shown in this figure, both schemes perform very well. The hump at both the exit as well as the re-entry is clearly resolved with no noticeable numerical artefacts or reflections.

Grid size	$SBP2$	rate	$SBP4$	rate
10×10	2.5×10^{1}		1.1×10^{1}	
20×20	5.8×10^{0}	2.1	1.5×10^{0}	2.9
40×40	1.3×10^{0}	2.0	1.6×10^{-1}	3.3
80×80	3.0×10^{-1}	2.0	1.6×10^{-2}	3.2
160×160	7.4×10^{-2}	2.0	1.9×10^{-3}	3.1

Table 2.4.6: Numerical experiment 2: Relative percentage errors for $|\mathbf{B}|$ in l^2 and rates of convergence for both $SBP2$ and $SBP4$.

Grid size	$SBP2$	rate	$SBP4$	rate
10×10	6.4×10^{-1}		9.7×10^{-2}	
20×20	3.9×10^{-1}	0.7	2.4×10^{-2}	2.0
40×40	9.1×10^{-2}	2.2	1.9×10^{-3}	3.6
80×80	2.6×10^{-2}	1.8	3.0×10^{-4}	2.7
160×160	8.9×10^{-3}	1.6	5.1×10^{-5}	2.5

Table 2.4.7: Numerical experiment 2: Divergence (errors) in l^2 and rates of convergence for both $SBP2$ and $SBP4$ at time $t=2\pi$.

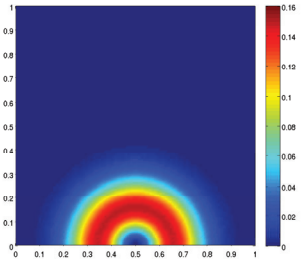

(a) SBP2, $t = \pi/2$

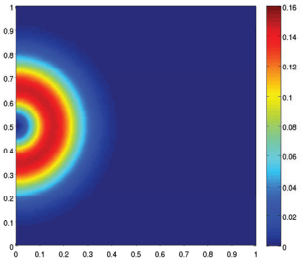

(b) SBP2, $t = 2\pi$

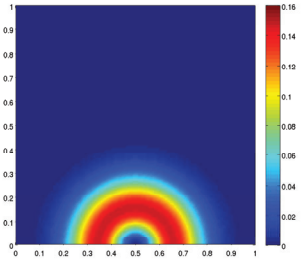

(c) SBP4,$t = \pi/2$

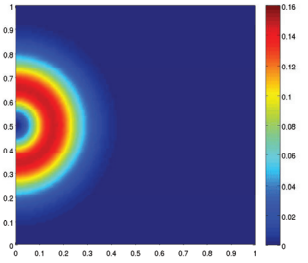

(d) SBP4,$t = 2\pi$

Figure 2.4.3: Numerical results for experiment 2. Mesh size 100×100.

As shown in Table 2.4.6, the errors are low after one full rotation for both the $SBP2$ and $SBP4$ schemes. In fact, the size of relative errors is lower than in the previous numerical experiment. As expected, the rates of convergence tend to 2 and 3 for $SBP2$ and $SBP4$ respectively. In Table 2.4.7 the divergence errors and their convergence rates are listed. They are small and the convergences approach the expected values 1.5 and 2.5.

On the other hand, when we tried to compute this example with the divergence preserving TF and $TF2$ schemes, the solution blew up on account of boundary instabilities.

Numerical Experiment 3: (Discontinuous solutions.) As remarked earlier, the magnetic induction equations (2.2.1) are a sub-model in the nonlinear MHD equations. As a consequence, one must solve the induction equation with both discontinuous velocity fields and initial data. It is therefore interesting to see how well the SBP-SAT schemes handle discontinuous velocity fields and initial data.

The SBP operators use centered finite differences in the interior. It is well known that using central differences leads to oscillations around discontinuities. Therefore the SBP schemes cannot be used directly in this regime, see [12] for details. To calculate solutions with discontinuities, one adds a small amount of explicit numerical diffusion that retain the accuracy of the first derivative SBP approximations as well as maintain the energy stability of the SBP scheme. We will use these operators together with the $SBP2$ and $SBP4$ schemes in order to compute discontinuous solutions of the magnetic induction equations.

The second-order (fourth-order) SBP operator for the first derivative with a second-order (fourth-order) numerical diffusion operator gives an approximation which is formally second-order (fourth-order) accurate in the interior of the computational domain. It turns out that a different scaling (dividing by the mesh size) of the numerical diffusion operator leads to a first order (third-order) "upwind" scheme. We will test all these numerical diffusion operators a numerical experiment first described in [5].

The computational domain is $[0,1] \times [0,1]$. Consider the constant velocity field, $\mathbf{u} = (1,2)^T$ and the discontinuous initial data,

$$B_0^1(x,y) = B_0^2(x,y) = \begin{cases} 2 & \text{if } x > y, \\ 0 & \text{otherwise.} \end{cases}$$

In this case, the exact solution (see [5]) of (5.1.1) reads

$$\mathbf{B}(x,y,t) = \mathbf{B}_0(x-t, y-2t).$$

The initial discontinuity simply moves along the diagonal of the domain. We use the exact solution restricted to the boundary as the Dirichlet boundary data. Tests with generic SBP-SAT schemes, (2.3.1), showed that the approximate solutions were very oscillatory, and we damp these oscillations by adding numerical diffusion.

We test the $SBP2$ ($SBP4$) scheme with the standard second-order (fourth-order) numerical diffusion operator as well as the scaled numerical diffusion operator to obtain the first-order (third-order) $SBP1$ and $SBP3$ schemes. The results on a 100×100 mesh at time $t = 0.5$ are plotted in Figure 2.4.4. A plot at this time is of interest as some part of the solution has interacted with the boundary and exited the domain, whereas

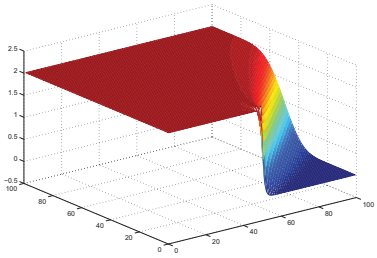

(a) $SBP1$

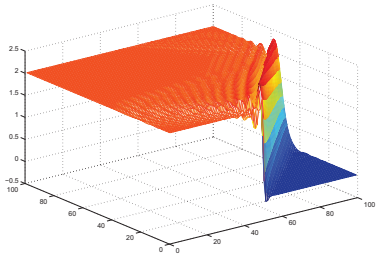

(b) $SBP2$, second-order diffusion

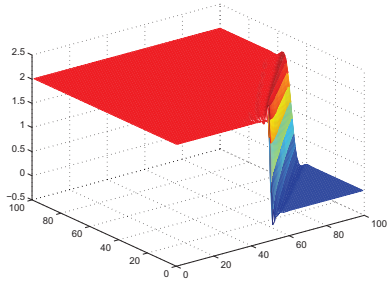

(c) $SBP3$

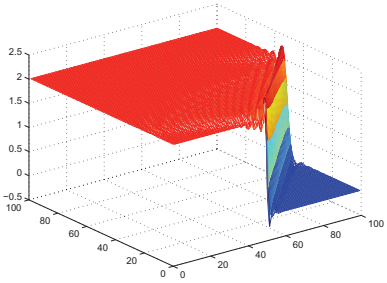

(d) $SBP4$, fourth-order diffusion

Figure 2.4.4: Numerical results for $B^1(x, y, 0.5)$ in experiment 3.

most of the front is still inside the domain. From Figure 2.4.4, we see that the boundary discretization works well in all cases and does not lead to any significant oscillations in the domain. The $SBP1$ scheme is the most dissipative with significant smearing at the discontinuity. However, this scheme also has no over/under shoots or oscillations and the solution is TVD. The $SBP2$ scheme with second-order numerical diffusion operator is oscillatory near the discontinuity with dispersive waves on both sides of it. The smearing is considerably less than that of the $SBP1$ scheme. The $SBP4$ scheme with standard fourth-order numerical diffusion is even more oscillatory and leads to a larger overshoot. The $SBP3$ scheme damps these oscillations somewhat and still keeps the sharpness at the discontinuity making it an acceptable alternative.

2.5 Conclusion

We have considered the magnetic induction equations that arise as a submodel in the MHD equations of plasma physics. Various forms of these equations were presented including the symmetric forms that are well-posed with general initial data and Dirichlet boundary conditions.

Standard numerical methods of the finite difference/finite volume type have dealt with discretizations of the constrained form (2.1.3) and attempted to preserve some form of the divergence constraint.

We describe SBP-SAT based finite difference schemes for the initial- boundary value problem corresponding to the magnetic induction equations. These schemes were based on the non-conservative symmetric form (2.1.4) and use SBP finite difference operators to approximate spatial derivatives and a SAT technique for implementing boundary conditions. The resulting schemes were energy stable and higher order accurate.

These schemes were tested on a series of numerical experiments, which illustrated their stability and high-order of accuracy. Interesting solution features were resolved very well. The fourth-order scheme was found to be well suited for long time integration problems. Despite the fact that the schemes were not preserving any particular form of discrete divergence as well as the lack of a rigorous discrete divergence bound, the divergence errors generated by the schemes were quite low and converged to zero at the expected rates when the mesh was refined. The schemes were compared with two existing lower order schemes and one divergence preserving second order scheme. Despite lacking any divergence bounds, the SBP schemes performed at least as well as the schemes with a divergence bound.

The numerical experiments indicate that the SBP-SAT framework is effective in approximating solutions of the magnetic induction equations to a high order of accuracy. In the future we plan to extend these schemes to magnetic induction equations with resistivity.

Bibliography

[1] D.S. Balsara and D. Spicer. A staggered mesh algorithm using high order Godunov fluxes to ensure solenoidal magnetic fields in magnetohydrodynamic simulations. *J. Comp. Phys.*, 149(2):270-292, 1999.

[2] N. Besse and D. Kröner. Convergence of the locally divergence free discontinuous Galerkin methods for induction equations for the 2D-MHD system. *M2AN Math. Model. Num. Anal* 39(6):1177-1202, 2005.

[3] J.U. Brackbill and D.C. Barnes. The effect of nonzero div$B$ on the numerical solution of the magnetohydrodynamic equations. *J. Comp. Phys.*, 35:426-430, 1980.

[4] W. Dai and P.R. Woodward. A simple finite difference scheme for multi-dimensional magnetohydrodynamic equations. *J. Comp. Phys.*, 142(2):331-369, 1998.

[5] C. Evans and J.F. Hawley. Simulation of magnetohydrodynamic flow: a constrained transport method. *Astrophys. J.*, 332:659, 1998.

[6] F. Fuchs, K.H. Karlsen, S. Mishra and N.H. Risebro. Stable upwind schemes for the Magnetic Induction equation. *Preprint,* Submitted.

[7] F. Fuchs, S. Mishra and N.H. Risebro. Splitting based finite volume schemes for ideal MHD equations. *in press Jl. Comput. Phys.,*

[8] S.K. Godunov. The symmetric form of magnetohydrodynamics equation. *Num. Meth. Mech. Cont. Media*, 1:26-34, 1972.

[9] B. Gustafsson, H.-O. Kreiss, and J. Oliger. *Time dependent problems and difference methods.* John Wiley & Sons, Inc., 1995.

[10] H.O. Kreiss and J. Lorenz. Initial-Boundary value problems and the Navier–Stokes equations. *Academic Press,* Boston, 1989.

[11] R.J. LeVeque. Finite volume methods for hyperbolic problems. *Cambridge university press,* Cambridge, 2002.

[12] K. Mattsson, M. Svärd and J. Nordström. Stable and Accurate Artificial Dissipation. *Journal of Scientific Computing*, Vol.21,No.1, August 2004.

[13] K. Mattsson and J. Nordström. Summation by parts operators for finite difference approximations of second derivative. *Journal of Computational Physics*, 199(2004), 503-540.

[14] S. Mishra and M. Svärd. On stability of numerical schemes via frozen coefficients and magnetic induction equations. *Preprint*, Submitted.

[15] J. Nordström. Error Bounded Schemes for Time-dependent Hyperbolic Problems *SIAM J. Sci. Comput.*, 30(2007), 46-59.

[16] J. Nordström and M. H. Carpenter High-Order Finite Difference Methods, Multidimensional Linear Problems, and Curvilinear Coordinates *J. Comput. Phys*, 173(2001), 149-174.

[17] K.G. Powell. An approximate Riemann solver for magneto-hydro dynamics (that works in more than one space dimension). Technical report, 94 -24, ICASE, Langley, VA, 1994.

[18] K.G. Powell, P.L. Roe. T.J. Linde, T.I. Gombosi and D.L. De Zeeuw, A solution adaptive upwind scheme for ideal MHD. J. Comp. Phys, 154(2), 284 - 309, 1999

[19] J. Rauch. *Partial Differential Equations*, Springer, 1991.

[20] D.S. Ryu, F. Miniati, T.W. Jones and A. Frank. A divergence free upwind code for multidimensional magnetohydrodynamic flows. *Astrophys. J.*, 509(1):244-255, 1998.

[21] M. Svärd On coordinate transformations for summation-by-parts operators *J. Sci. Comput.* 20(2004), 29-42.

[22] M. Svärd and J. Nordström. On the order of accuracy for difference approximations of initial-boundary value problems. *Journal of Computational Physics*, 218(2006), 333-352.

[23] M. Torrilhon and M. Fey. Constraint-preserving upwind methods for multidimensional advection equations. *SIAM. J. Num. Anal.*, 42(4):1694-1728, 2004.

[24] G. Toth. The div$B = 0$ constraint in shock capturing magnetohydrodynamics codes. *J. Comp. Phys.*,161:605-652, 2000.